| 1. Report No. | 2. Government Accession No. | 3. Recipient's Catalog No. |
|---|---|---|
| FHWA/TX-05/9-1520-P2 | | |

| 4. Title and Subtitle | 5. Report Date |
|---|---|
| DESIGN, CONSTRUCTION, AND MAINTENANCE OF BRIDGE DECKS UTILIZING GFRP REINFORCEMENT | February 2005 |
| | 6. Performing Organization Code |
| 7. Author(s) | 8. Performing Organization Report No. |
| David Trejo, Francisco Aguiñiga, Ray W. James, and Peter B. Keating | Product 9-1520-P2 |
| 9. Performing Organization Name and Address | 10. Work Unit No. (TRAIS) |
| Texas Transportation Institute<br>The Texas A&M University System<br>College Station, Texas 77843-3135 | 11. Contract or Grant No.<br>Project 9-1520 |
| 12. Sponsoring Agency Name and Address | 13. Type of Report and Period Covered |
| Texas Department of Transportation<br>Research and Technology Implementation Office<br>P. O. Box 5080<br>Austin, Texas 78763-5080 | Product |
| | 14. Sponsoring Agency Code |

15. Supplementary Notes

Project performed in cooperation with the Texas Department of Transportation and the Federal Highway Administration.
Project Title: FRP Reinforcing Bars in Bridge Decks
URL: http://tti.tamu.edu/documents/9-1520-P2.pdf

16. Abstract

Fiber-reinforced polymers (FRP) are being increasingly used in the construction industry. One application is to use FRP bars as reinforcement in concrete. Because glass fiber-reinforced polymer (GFRP) bars are now being used, guidance is needed on how to design, construct, and maintain reinforced concrete structures containing this reinforcement. This report provides a discussion of design issues related to GFRP-reinforced bridge decks and is followed by a design example. Recommendations for possible modifications to the 1998 American Association of State Highway Officials (AASHTO) LRFD Bridge Design Specifications are provided. In addition, some guidelines on the construction and maintenance of GFRP-reinforced systems are provided. It should be noted that more research and field work is needed to provide standardize guidelines. This report provides guidance using the information available and the user should use sound engineering judgment in the design, construction, and maintenance of GFRP-reinforced structures.

| 17. Key Words | 18. Distribution Statement |
|---|---|
| GFRP, Strength, Design, Construction, Maintenance, Strength Deterioration. | No restrictions. This document is available to the public through NTIS:<br>National Technical Information Service<br>Springfield, Virginia 22161<br>http://www.ntis.gov |

| 19. Security Classif.(of this report) | 20. Security Classif.(of this page) | 21. No. of Pages | 22. Price |
|---|---|---|---|
| Unclassified | Unclassified | 72 | |

# DESIGN, CONSTRUCTION, AND MAINTENANCE OF BRIDGE DECKS UTILIZING GFRP REINFORCEMENT

by

David Trejo, PhD
Associate Professor and Associate Researcher
Texas A&M University and Texas Transportation Institute

Francisco Aguiñiga, PhD
Assistant Professor
Texas A&M University Kingsville

Ray W. James, PhD
Associate Professor and Manager, Highway Structures Program
Texas A&M University and Texas Transportation Institute

and

Peter B. Keating, PhD
Associate Professor and Associate Researcher
Texas A&M University and Texas Transportation Institute

Product 9-1520-P2
Project Number 9-1520
Project Title: FRP Reinforcing Bars in Bridge Decks

Performed in Cooperation with the
Texas Department of Transportation
and the
Federal Highway Administration

February 2005

TEXAS TRANSPORTATION INSTITUTE
The Texas A&M University System
College Station, Texas 77843-3135

# DISCLAIMER

The contents of this report reflect the views of the authors, who are responsible for the facts and the accuracy of the data presented herein. The contents do not necessarily reflect the official view or policies of the Federal Highway Administration (FHWA) or the Texas Department of Transportation (TxDOT). This report does not constitute a standard, specification, or regulation. The researcher in charge of the project was Dr. David Trejo.

# ACKNOWLEDGMENTS

This project was performed in cooperation with the Federal Highway Administration and the Texas Department of Transportation. This report was written by Drs. David Trejo, Francisco Aguiñiga, Ray W. James, and Peter B. Keating. Financial support for the research was provided by the Federal Highway Administration, Texas Department of Transportation, and the Texas Transportation Institute.

The authors wish to express their gratitude to:

Project Coordinator:
Ronald E. Koester, P.E., TxDOT, Waco District

Project Director:
Timothy E. Bradberry, P.E., TxDOT, Bridge Division

Project Advisors:
Don Harley, P.E., Federal Highway Administration
Mary Lou Ralls, P.E., Retired State Bridge Engineer, TxDOT
Joe Chappell, P.E., TxDOT, Amarillo District
Mark Bloschock, P.E., TxDOT, Bridge Division
Kevin Pruski, P.E., TxDOT, Bridge Division
Robert Sarcinella, TxDOT, Construction Division
Paul McDad, TxDOT, Construction Division
Tom Yarbrough, TxDOT, Research Division

# TABLE OF CONTENTS

# LIST OF FIGURES

# LIST OF TABLES

**Table** **Page**

# I. INTRODUCTION

Corrosion of steel reinforcement embedded in concrete transportation structures results in significant costs and negatively impacts the traveling public. Researchers and engineers have been searching for alternative materials that do not exhibit the typical expansion of the steel corrosion products that result in cracking and spalling of the concrete cover. These cracks and spalls reduce the integrity of the reinforced concrete structure and can significantly reduce the ride quality of the concrete bridge deck. Corrosion of fiber-reinforced polymers (FRP) does not exhibit expansion of the corrosion product and has been identified as a potential material for use in reinforced concrete structures. This report provides guidance on the design, construction, and maintenance of bridge decks reinforced with glass fiber-reinforced polymer (GFRP) concrete reinforcement. This report reviews the American Concrete Institute (ACI) 440.1R-03 (2003), *Guide for the Design and Construction of Concrete Reinforced with FRP Bars* (herein referred to as the ACI 440.1R-03 design and construction guidelines), and suggests modifications as needed. The report also provides proposed revisions to the 1998 American Association of State Highway and Transportation (AASHTO) Load and Resistance Factor Design (LRFD) *Bridge Design Specifications*. Recommended construction and maintenance guidelines for GFRP-reinforced concrete are also provided.

It should be noted that many issues related to the use of GFRP reinforcement require further research; the results presented here are from Report 9-1520-3 *Characterization of Design Parameters for Fiber Reinforced Polymer Composite Systems,* by Trejo et al. (2003). It should also be noted that the three materials evaluated in Report 9-1520-3 were from a single lot from each of three manufacturers. It was assumed that the materials from these single lots and manufacturers represent of the GFRP materials present in industry. The reader and/or user must use good judgment and engineering when applying the following recommendations.

## II. ACI 440.1R-03 DESIGN GUIDELINES: REVIEW AND PROPOSED MODIFICATIONS

This section reviews the ACI 440.1R-03 design and construction guidelines (2003) as they relate to the results obtained in the research reported in Report 9-1520-3 (Trejo et al. 2003). The ACI 440.1R-03 design and construction guidelines present information on the history and use of fiber-reinforced polymer (FRP) reinforcement, a description of the material properties of FRP, and committee recommendations relative to the construction of concrete structures reinforced with FRP bars. This document also includes recommended material requirements, construction practices, and design recommendations. Only those sections of the ACI 440.1R-03 design and construction guidelines that the researchers believe could be improved and are related to the use of glass fiber-reinforced polymer (GFRP) bars in bridges are reviewed.

The first section of the ACI 440.1R-03 design and construction guidelines to be reviewed is Section 7.2, Design Material Properties, specifically as related to the environmental reduction factors proposed by the guidelines to be applied to the tensile strength of FRP bars reinforced with glass fibers. A review of Section 8.3, Serviceability, follows. The serviceability section review includes cracking (subsection 8.3.1) and deflections (addressed in subsections 8.3.2 and 8.3.2.3). Section 11.1, regarding the development length of straight bars, is also reviewed. Finally, comments are provided in regard to minimum concrete cover.

### ACI 440.1R-03 SECTION 7.2 DESIGN MATERIAL PROPERTIES

Section 7.2 of the guidelines indicates that the material properties provided by the manufacturer should be reduced to account for long-term environmental exposure.

The guidelines recommend that the tensile strength should be determined by:

$$f_{fu} = C_E f^*_{fu} \quad (1)$$

where,

$f_{fu}$ = Design tensile strength of FRP, considering reduction for service environment (*ksi*),

$C_E$ = Environmental reduction factor,

$f^*_{fu}$ = Guaranteed tensile strength of an FRP bar defined as the mean tensile strength of a sample of test specimens minus three times the standard deviation ($f^*_{fu} = f_{u,ave} - 3\sigma$) (*ksi*),

$f_{u,ave}$ = Average tensile strength of FRP bars.

The environmental reduction factors given in the guidelines for GFRP bars are 0.8 and 0.7 for concrete not exposed to earth and weather and for concrete exposed to earth and weather, respectively. The guidelines indicate that the environmental reduction factors are conservative estimates that account for temperature effects, as long as the material is not used at temperatures higher than the glass transition temperature of the polymer employed to manufacture the bars.

The average tensile strengths of the unexposed specimens of the tension tests in Report 9-1520-3 (Trejo et al. 2003) are presented in column 2 of Table 1. The unexposed tensile strengths, standard deviations, and guaranteed tensile strengths are shown in columns 3 and 4, respectively, of Table 1. Also shown in columns 5 and 6 of Table 1 are the design tensile strengths computed using Equation 1. The smallest measured tensile strength from any of the exposure conditions at 50 weeks is shown in column 7 of Table 1. Column 8 shows the guaranteed tensile strength ($f^*_{fu} = f_{u,ave} - 3\sigma$) obtained from the measured exposure data at 50 weeks. Column 9 presents the predicted average residual tensile strength computed using a value of $\lambda = 0.0057$ (best fit to guaranteed tensile strength) computed using the method described in the tensile strength degradation analysis section of the moisture absorption test results in Report 9-1520-3 (Trejo et al. 2003), for a five-year exposure period. Column 10 shows the predicted

residual tensile strength using a value of λ = 0.006 (curve fit to lowest measured data points) described in the tensile strength degradation analysis section of the moisture absorption test results in Report 9-1520-3 (Trejo et al. 2003), for a five-year exposure period.

According to comparisons made with the research conducted by Sen et al. (2002) as discussed in Report 9-1520-3 (Trejo et al. 2003) in the tensile strength degradation analysis section, the results predicted that a value of λ 0.0057 (best fit to guaranteed tensile strength) can be considered as the upper bound residual tensile strengths. The predictions are considered as upper bound residual strength values because the bars were exposed unstressed, and as indicated by Sen et al., the application of a sustained stress to GFRP bars causes larger strength reductions with time when the bars are unstressed.

**Table 1. Tensile Strength Results and Predicted Values.**

| Bar type | Tensile strength (psi) | | | | | Smallest 50 weeks $f_u$ (psi) | Guaranteed 50 weeks $f^*_{fu}$ (psi) | Predicted 5 years $f^*_{fu}$ (psi) | Predicted 5 years $f_u$ (psi) |
|---|---|---|---|---|---|---|---|---|---|
| | $f_{u,\,avg}$ unexp. | S.D. unexp. | $f^*_{fu}$ unexp. | $f_{fu}$ ($C_E$ =0.8) | $f_{fu}$ ($C_E$ =0.7) | | | | |
| (1) | (2) | (3) | (4) | (5) | (6) | (7) | (8) | (9) | (10) |
| P | 84,588 | 2,456 | 77,219 | 61,775 | 54,053 | 68,616 | 59,995 | 52,868 | 53,798 |
| V1 | 88,507 | 7,951 | 64,655 | 51,724 | 45,258 | 70,969 | 63,559 | 55,317 | 56,290 |
| V2 | 74,471 | 2,598 | 66,676 | 53,341 | 46,673 | 56,609 | 54,863 | 46,544 | 47,363 |

Comparing the values presented in columns 6 and 8 of Table 1 shows that the values of column 6 are only 11, 40, and 18 percent lower than the values of column 8. The values of $f_{fu}$ represent the design tensile strength obtained following ACI 440.1R-03, and include an environmental reduction factor for exterior exposure that is intended to account for strength reductions suffered by GFRP bars over the life of the structure. The results shown indicate that the design strength is slightly larger than the guaranteed tensile strength after only one year of exposure for bar type P. Since the reductions in strength shown in column 8 were determined for unstressed specimens, it is expected that the guaranteed tensile strength will be lower in actual service conditions, where the GFRP bars are stressed.

A comparison of columns 6 and 9 of Table 1 show that the five-year predicted guaranteed tensile strengths are equivalent to 0.98, 1.22, and 1.00 of the design strengths presented in column 6. This indicates that the GFRP bars evaluated in the research can have a guaranteed residual tensile strength close to the design strength after only five years of unstressed exposure. As already noted, GFRP bars are expected to have a lower residual tensile strength when they are stressed in service conditions.

Glaser et al. (1983) conducted a 10-year study on the life estimation of S glass/epoxy composites under sustained tensile load. The specimens were kept at a temperature between 68 °F and 82 °F and a relative humidity between 24 and 37 percent. The researchers found that the residual tensile strength of the specimens continuously decreased with time, even beyond five years, at these relatively low humidity levels. Based on the observations reported in 9-1520-3 (Trejo et al. 2003) and because the tensile strength of GFRP bars in stressed service conditions is expected to either level off or continue to degrade after one year of exposure, the results indicate that the environmental reduction factors given by the ACI 440.1R-03 design and construction guidelines may not be conservative.

As indicated in the tensile strength degradation analysis section of the moisture absorption test shown in Report 9-1520-3 (Trejo et al. 2003), it is difficult to make valid predictions for long periods of time with the limited exposure times studied. It is therefore necessary to carry out exposure tests over longer periods of time to make reliable long-term behavior predictions.

The application of the strength reduction factors is presented in a design example later.

## ACI 440.1R-03 SECTION 8.3.1 CRACKING

The ACI 440.1R-03 design and construction guidelines indicate that FRP bars are corrosion resistant and, as a result, the maximum crack width limitation can be relaxed when corrosion of the reinforcement is the main reason for crack-width

limitations. The guidelines recommend using maximum crack width limits of 0.02 inch for exterior exposure and 0.028 inch for interior exposure.

The results section of the cracking of the concrete slabs test in Report 9-1520-3 (Trejo et al. 2003) indicated that maximum crack width increases with concrete cover. However, as indicated by Beeby (1978), although the crack width on the surface of the concrete is a function of concrete cover, the crack width at the level of the reinforcement could be approximately the same. Thus, it would be better to specify a maximum surface crack width limit that is a function of concrete cover if the degradation of the GFRP bar depends on the crack width at the surface of the bar rather than at the surface of the concrete. However, until research that relates the degradation of GFRP bars to crack width at the surface of the concrete and at the surface of the GFRP bar is available, no recommendations can be made.

The ACI 440.1R-03 design and construction guidelines recommend using Equation 8-9b (or 8-9c) to estimate the maximum crack width of FRP-reinforced concrete elements. As described in the results section for the cracking of concrete slabs test in Report 9-1520-3 (Trejo et al. 2003), the following expression yields a good fit to the experimental data:

$$W_{\max} = 0.09\beta \cdot f_f \cdot \sqrt[3]{d_c A} \qquad (2)$$

where,

$W_{max}$ = most probable maximum crack width

$\beta$ = $h_2/h_1$,

$h_1$ = Distance from the centroid of the reinforcement to the neutral axis (*inch*),

$h_2$ = Distance from the extreme tension fiber to the neutral axis (*inch*),

$f_f$ = Stress in the reinforcement (*ksi*),

$d_c$ = Bottom cover measured from the center of lowest bar (*inch*),

$A$ = Twice the difference between the total and effective depths multiplied by the width of the section (effective area of concrete surrounding the main reinforcement) divided by the number of bars ($inch^2$).

Figure 1 compares Equation 2 with ACI 440.1R-03 Equation 8-9b, the equation proposed by Faza and GangaRao (1993), and the experimental data obtained from this research. Note that the equation by Faza and GangaRao is more conservative, but past practice has been to use the best-fit line equation instead of the more conservative approach. The ACI 440.1R-03 maximum crack width limit for exterior exposure is also shown in Figure 1.

According to the analysis presented in Section IV of the 9-1520-3 report (Trejo et al. 2003) in the cracking of concrete slabs test results section, Equation 2 yields a good prediction of average maximum crack width and a better prediction than the work done by Faza and GangaRao (1993). Previous to this research, limited test results were available on maximum crack width of FRP-reinforced concrete elements, and limited analysis had been performed to evaluate the correlation between test data and proposed equations. It should be noted that Equation 2 was developed based on experiments on slabs only.

An application of Equation 2 is presented in the design example given later. The example presents the maximum crack width computations obtained using Equation 2 and ACI 440.1R-03 Equations 8-9b and 8-9c shown next as Equations 3 and 4, respectively:

$$W_{\max} = 0.076\beta \cdot \frac{E_s}{E_f} f_f \cdot \sqrt[3]{d_c A} \tag{3}$$

$$W_{\max} = \frac{2200}{E_f} \beta \cdot k_b f_f \cdot \sqrt[3]{d_c A} \tag{4}$$

where

$E_s$ = modulus of elasticity of steel (29,000 *ksi*),

$E_f$ = modulus of elasticity of FRP bars (ksi),

$k_b$ = bond modification factor with a recommended value of 1.2 for bond strength between FRP bars and concrete (similar to the bond strength between steel bars and concrete),

all other terms were previously defined.

The results of the design example show that Equations 2 and 4 yield similar maximum crack widths. In addition, the maximum crack widths obtained with Equations 2 and 4 are larger, and therefore more conservative, than those obtained with Equation 3.

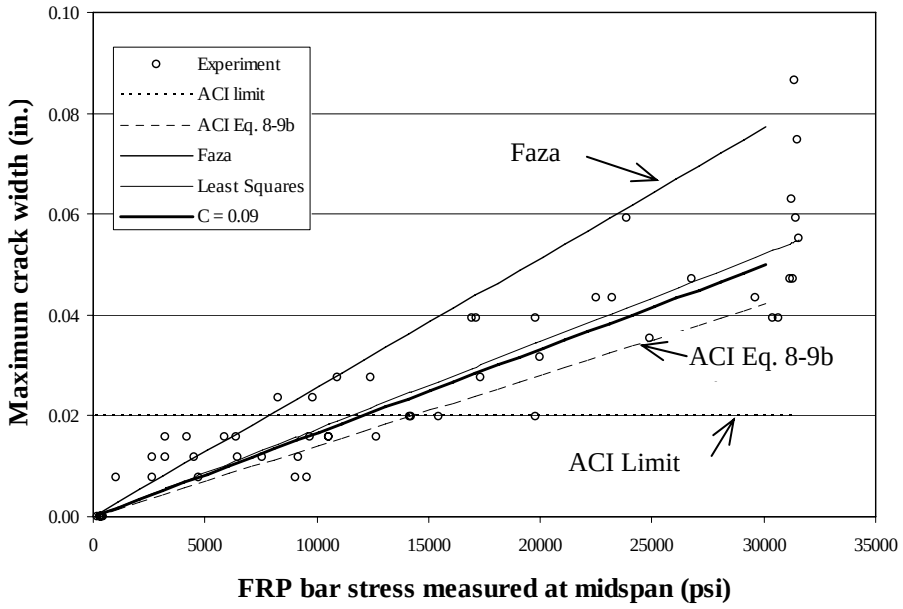


**Figure 1. Crack Comparisons for a 1.21-Inch Concrete Cover.**

## ACI 440.1R-03 SECTION 8.3.2 DEFLECTIONS

The ACI 440.1R-03 design and construction guidelines require that deflections be limited in FRP-reinforced concrete flexural members. The guidelines follow the deflection limitations of the ACI 318 building code (2000), in which the deflections of reinforced concrete elements under immediate and sustained static loads are limited. However, the deflection limitations of the ACI 440.1R-03 design and construction guidelines and the ACI 318 code do not apply to dynamic loads, such as earthquakes, transient winds, or vibration of machinery.

The results of the research reported in Report 9-1520-3 (Trejo et al. 2003) on the cyclic loading of concrete beam tests indicate that the deflections of beams subjected to 2 million cycles of loading with a GFRP bar stress range of 18.9 ksi increased by 78 percent. This increment was computed from a least-squares best-fit line to the data. Therefore, the deflection increase due to cyclic loading is significant and should be accounted for in the ACI 440.1R-03 design and construction guidelines. In the absence of more test data, the following equation can be used to estimate a lower bound of the increase in long-term deflections due to cyclic loading:

$$y = 0.0046\ln(n) + 0.0858 \quad (5)$$

Where,

$y$ = beam deflection in inches,

$n$ = the number of cycles.

The correlation coefficient between beam deflection and the number of cycles is $R^2$ = 0.47. The slope of this equation can be used to compute deflections due to cyclic loading of GFRP-reinforced concrete members.

An application of Equation 5 to estimate deflections due to cyclic loading is shown in the example presented later. The design example computes the deflections of a GFRP-reinforced concrete beam subjected to dead load and the application of 2 million cycles of an alternating live load. The results show an initial deflection due to dead and live load of 0.37 inches and a final deflection due to dead and live load of 0.47 inches after 2 million cycles of the live load. This represents a 27 percent increase in deflection due to cyclic load application.

## ACI 440.1R-03 SECTION 8.3.3 CALCULATION OF DEFLECTION (DIRECT METHOD)

This section of the ACI 440.1R-03 design and construction guidelines presents a method to compute long-term deflections of FRP-reinforced concrete elements using ACI 440.1R-03 Equation 8-14:

$$\Delta_{(cp+sh)} = 0.6\xi(\Delta_i)_{sus} \quad (6)$$

where,

$\Delta_{(cp+sh)}$ = Additional deflection due to creep and shrinkage under sustained loads (*mm, inch*)

$(\Delta i)_{sus}$ = Immediate deflection due to sustained loads (service loads) (*mm, inch*)

$\xi$ = Time-dependent factor for sustained load defined in the ACI 318 building code (2000)

Equation 6 can predict smaller deflections than measured. Perhaps the biggest advantage of Equation 6 is its simplicity. However, this equation does not specifically account for creep of FRP bars. The method described in the creep section of Section IV of the 9-1520-3 report for the computation of long-term deflection of GFRP-reinforced concrete elements, which accounts for creep of GFRP bars, is proposed as an alternative to Equation 6. The following equation can be used to compute the increment in curvature:

$$\Delta\kappa = \frac{B_e\delta N - A_e^{'}\delta M}{E_e\left(B_e^{\,2} - A_e I_e\right)} \quad (7)$$

and the following equation can be used to compute the long-term deflection:

$$y_C = \frac{L^2}{96}\left(\kappa_A + 10\kappa_C + \kappa_B\right) \quad (8)$$

where,

$A_e$ = area of the age-adjusted transformed section,

$B_e$, = first moment of the age-adjusted transformed section about the top surface,

$I_e$ = second moment of the age-adjusted transformed section about the top surface, respectively.

$\kappa_{A,}\ \kappa_B$ = curvatures at the supports,

$\kappa_C$ = curvature at midspan.

$A_e$, $B_e$, and $I_e$ are the properties of the transformed area obtained using the age-adjusted effective modulus, $E_e$, in the computation of the transformed area of the bonded reinforcement.

Long-term deflection computations obtained with Equations 7 and 8 for a beam with a 14 foot span are shown in the design example. The six-month dead load deflections obtained with Equation 6 are 0.2 inches, and the six-month dead load deflections obtained with Equations 7 and 8 are 0.61 inches. Thus, the six-month deflection due to dead load computed with the newly proposed method from this research is equal to three times the deflection obtained with Equation 8-14 from the ACI 440.1R-03 design and construction guidelines.

## ACI 440.1R-03 SECTION 11.1 DEVELOPMENT LENGTH OF A STRAIGHT BAR

The development length of a straight bar can be computed with Equation 11-3 of the ACI 440.1R-03 design and construction guidelines as follows:

$$l_{bf} = \frac{d_b f_{fu}}{4\mu_f} \tag{9}$$

where,

$l_{bf}$ = Basic development length (*inch*),

$d_b$ = Bar diameter (*inch*),

$f_{fu}$ = Design tensile strength of FRP, considering reductions for service environment (*ksi*),

$\mu_f$ = Bond strength between FRP bar and concrete (*ksi*).

The bond test results presented in Section IV of Report 9-1520-3 (Trejo et al. 2003) indicate that the bond strength of GFRP bars exposed to an environment with high temperature and moisture was lower than the bond strength of specimens exposed outdoors. In addition, the number of specimens exposed to controlled conditions that failed by pullout was twice the number of specimens from the outdoor exposure group that experienced pullout failures. However, this research included only a small number of samples. The displacement recorded at the loaded end was larger, on average, for the specimens exposed in temperature- and moisture-controlled conditions than for the specimens exposed outdoors. These displacements are indications that bond strength degrades over time. ACI 440.1R-03 Equation 11-3 recognizes that the tensile strength of GFRP bars degrades with time and yields a smaller development length for a smaller tensile strength. Nevertheless, when the bond strength degrades, the development length increases. This fact may make Equation 9 unconservative. The development length of Equation 9 should depend on the ratio of the rate of tensile strength degradation of GFRP bars to the rate of bond strength degradation between the GFRP bars and

concrete. Additional research is needed to better estimate both the rate of tensile strength degradation in a given environment and the rate of bond degradation in the same environment. Perhaps the simplest way to account for the bond strength degradation would be to apply an environmental reduction factor to the bond strength.

The bond strength of FRP bars in concrete depends on the compressive strength of concrete, and tests have determined the denominator of Equation 9 to be approximately 2.85 ksi. The ACI 440.1R-03 design and construction guidelines propose using Equation 11-7:

$$l_{bf} = \frac{d_b f_{fu}}{2700} \tag{10}$$

where, $f_{fu}$ is the design tensile strength of GFRP. If the basic development length of an FRP bar is computed with this equation, the bar should have adequate development length at the end of its service life, since this equation includes an environmental reduction factor ($C_E$) in $f_{fu}$. But, the bond length should be sufficient to develop the full strength of the bar when the bar is put in service ($f_{u,ave}$), as well as the strength of the bar when it is close to the end of its service life ($f_{fu}$). Therefore, the basic development length obtained would be insufficient to develop the guaranteed tensile strength ($f^*_{fu} = f_{u,ave} - 3\ \sigma = f_{fu}/C_E$) or the average tensile strength ($f_{u,ave}$) of the GFRP bar when the structure is put in service.

Until sufficient data are available to determine the rate of degradation of the tensile strength and the rate of degradation of the bond strength, the average tensile strength should be used in the computation of the basic development length for GFRP bars, without reducing it by three standard deviations and without the application of the environmental reduction factor as shown in Equation 10. Thus, this research recommends that the following equation be used to compute the basic development length and should replace Equation 11-7 in the ACI 440.1R-03 design and construction guide (2003):

$$l_{bf} = \frac{d_b f_{u,ave}}{2700} \quad (11)$$

where the terms have already been defined.

A design example later shows the basic development lengths computed using Equations 10 and 11 for No. 6 FRP reinforcement. Equation 10 yields a basic development length of 17 inches and Equation 11 yields a basic development length of 26.4 inches. Thus, Equation 11 can yield basic development lengths 55 percent larger than those obtained with Equation 10 (ACI 440.1R-03 equation, 11-7).

## MINIMUM CONCRETE COVER

Results of the thermal expansion of the concrete slabs test indicate that using 0.75-inch diameter GFRP bars in 8-inch concrete bridge decks with clear covers of 1, 2, and 3 inches would not crack under a temperature increase of 54 °F from the concrete setting temperature for a concrete compressive strength of 5.88 ksi or higher. The fact that 0.75-inch diameter GFRP bars could be safely used in concrete elements subjected to temperature increases smaller than 54 °F for 1-, 2-, and 3-inch concrete covers could be used in the ACI 440.1R-03 design and construction guidelines to determine minimum concrete cover requirements. The concrete covers of 1, 2, and 3 inches are equivalent to 1.33, 2.66, and 4 bar diameters, respectively. From the results of this research it cannot be determined whether the minimum concrete cover of 1 bar diameter recommended by the ACI 440.1R-03 design and construction guidelines has problems with cracking due to thermal expansion. However, it can be concluded from the results of this research that a minimum concrete cover of 1.33 bar diameters would likely not cause thermal expansion and cracking of typical bridge decks under normal environmental conditions.

## INTRODUCTION TO DESIGN EXAMPLE

This section presents a design example that includes the recommended modifications and/or verifications to the ACI 440.1R-03 design and construction guidelines. A simply supported beam subjected to distributed dead and live loads is

designed for strength. The resulting design section is then checked to satisfy deflection, maximum crack width, and creep rupture stress limits. The basic development length is also computed. Finally, the beam deflections due to 2 million cycles of live load applications are estimated.

## DESIGN EXAMPLE

### Objective

Design a simply supported rectangular concrete beam with a span of 14 ft. The beam will be in the exterior of a structure. The beam should carry a service live load of $w_{LL}$ = 1.2 kip/ft and a superimposed dead load of $w_{SDL}$ = 0.6 kip/ft. The deflection of the beam at six months should not exceed $l$/240, and the instantaneous live load deflection should not exceed $l$/360. GFRP bars reinforce the beam. The average tensile strength of the GFRP bars is $f_{u,ave}$ = 96 ksi, the standard deviation is (S.D.) = 2.5 ksi, and the guaranteed tensile strength is $f^*_{fu}$ = 88.5 ksi. Other material properties are: $E_f$ = 6,279 ksi and $f_c'$ = 4 ksi. Assume the beam has adequate shear strength. Assume the beam will be cured for 7 days and first loaded at 14 days of age. Compute the basic development length of the GFRP reinforcement. Estimate the beam midspan deflection after 2 million cycles of loading due to an alternating live load. Figure 2 shows a design based on the modified ACI 440.1R-03 design and construction guidelines.

| Design based on ACI 440.1R-03 design guidelines | Design based on results from this research project |
|---|---|
| **1. Estimate the beam size.**<br><br>Estimate the depth of a simply supported reinforced concrete beam from Table 9.5(a) of the ACI 318 code. Deflections, however, need to be checked.<br>$h \cong \frac{l}{16}$<br>$h \cong \frac{(14\,ft)\left(12\,\frac{in.}{ft}\right)}{16} = 10.5\,in.$<br>Since GFRP bars have lower stiffness than steel bars, greater depth than steel-reinforced concrete may be required for deflection control<br><br>Try $h$ = 16 inches<br>Try $b$ = 10.5 inches | **1. Estimate the beam size.**<br><br>Estimate the depth of a simply supported reinforced concrete beam from Table 9.5(a) of the ACI 318 code. Deflections, however, need to be checked.<br>$h \cong \frac{l}{16}$<br>$h \cong \frac{(14\,ft)\left(12\,\frac{in.}{ft}\right)}{16} = 10.5\,in.$<br>Since GFRP bars have lower stiffness than steel bars, greater depth than steel-reinforced concrete may be required for deflection control<br><br>Try $h$ = 16 inches<br>Try $b$ = 10.5 inches |
| **2. Factored load**<br><br>Compute the distributed dead load: $w_{DL} = w_{SDL} + w_{SW}$ .<br>$w_{DL} = 600\,\frac{lb}{ft} + \frac{(10.5\,in.)(16\,in.)}{\left(12\,\frac{in.}{ft}\right)^2}(150\,pcf) = 775\,\frac{lb}{ft}$<br>Compute the total factored load $w_u = 1.4w_{DL} + 1.7w_{LL}$ .<br>$w_u = 1.4\left(0.775\,\frac{kip}{ft}\right) + 1.7\left(1.2\,\frac{kip}{ft}\right) = 3.13\,\frac{kip}{ft}$ | **2. Factored load**<br><br>Compute the distributed dead load: $w_{DL} = w_{SDL} + w_{SW}$ .<br>$w_{DL} = 600\,\frac{lb}{ft} + \frac{(10.5\,in.)(16\,in.)}{\left(12\,\frac{in.}{ft}\right)^2}(150\,pcf) = 775\,\frac{lb}{ft}$<br>Compute the total factored load $w_u = 1.4w_{DL} + 1.7w_{LL}$ .<br>$w_u = 1.4\left(0.775\,\frac{kip}{ft}\right) + 1.7\left(1.2\,\frac{kip}{ft}\right) = 3.13\,\frac{kip}{ft}$ |

**Figure 2: Design Example.**

| Design based on ACI 440.1R-03 design guidelines | Design based on results from this research project |
|---|---|
| **3. Compute the design strength.**<br>For a beam located in an exterior space an environmental reduction factor ($C_E$) of 0.7 is used. The design rupture strength is:<br>$f_{fu} = C_E f_{fu}^*$<br>$f_{fu} = (0.7)(88.5\ ksi) = 62.0\ ksi$ | **3. Compute the design strength.**<br>For a beam located in an exterior space an environmental reduction factor ($C_E$) of 0.70 is used. The design rupture strength is:<br>$f_{fu} = C_E f_{fu}^*$<br>$f_{fu} = (0.7)(88.5\ ksi) = 62.0\ ksi$ |
| **4. Determine the area of GFRP bars required for flexural strength.**<br>Factored moment demand at midspan:<br>$M_u = \frac{w_u l^2}{8}$<br>$M_u = \frac{\left(3.13 \frac{kip}{ft}\right)(14\ ft)^2}{8} = 76.6\ kip \cdot ft$<br>Balanced reinforcement ratio:<br>$\rho_{fb} = 0.85 \frac{f_c'}{f_{fu}} \beta_1 \frac{E_f \varepsilon_{cu}}{E_f \varepsilon_{cu} + f_{fu}}$<br>$\rho_{fb} = 0.85 \frac{4}{62.0}(0.85) \frac{(6279)(0.003)}{(6279)(0.003) + 62.0}$<br>$\rho_{fb} = 0.0109$<br>For a failure controlled by concrete crushing, the reinforcement ratio should be at least 1.4 $\rho_{fb.}$ If $\rho_f \geq 1.4\ \rho_{fb}$, the strength reduction factor is 0.70. | **4. Determine the area of GFRP bars required for flexural strength.**<br>Factored moment demand at midspan:<br>$M_u = \frac{w_u l^2}{8}$<br>$M_u = \frac{\left(3.13 \frac{kip}{ft}\right)(14\ ft)^2}{8} = 76.6\ kip \cdot ft$<br>Balanced reinforcement ratio:<br>$\rho_{fb} = 0.85 \frac{f_c'}{f_{fu}} \beta_1 \frac{E_f \varepsilon_{cu}}{E_f \varepsilon_{cu} + f_{fu}}$<br>$\rho_{fb} = 0.85 \frac{4}{62.0}(0.85) \frac{(6279)(0.003)}{(6279)(0.003) + 62.0}$<br>$\rho_{fb} = 0.0109$<br>For a failure controlled by concrete crushing, the reinforcement ratio should be at least 1.4 $\rho_{fb.}$ If $\rho_f \geq 1.4\ \rho_{fb}$, the strength reduction factor is 0.70. |

**Figure 2: Design Example. (Continued)**

| Design based on ACI 440.1R-03 design guidelines | Design based on results from this research project |
|---|---|
| $1.4\rho_{fb} = 0.0152$<br>Try using 6-No. 6 bars with a cover of 1.5 inch and No. 3 stirrups:<br>$d = 16\ in. - 1.5 - 0.375 - (0.743/2) = 13.75\ in.$<br>$A_f = 0.433\ in.^2 (6) = 2.60\ in.^2$<br>$\rho_f = \frac{A_f}{bd}$<br>$\rho_f = \frac{2.60\ in.^2}{10.5\ in.(13.75\ in.)} = 0.0180 > 1.4\rho_{fb} \therefore \phi = 0.7$<br><br>Find the FRP bar stress when the ultimate strain of 0.003 in the concrete is reached:<br>$f_f = \sqrt{\frac{(E_f \varepsilon_{cu})^2}{4} + \frac{0.85\beta_1 f_c'}{\rho_f} E_f \varepsilon_{cu}} - 0.5 E_f \varepsilon_{cu} \le f_{fu}$<br>$f_f = \sqrt{\frac{[6279(0.003)]^2}{4} + \frac{0.85(0.85)(4)}{0.0180}(6279)(0.003)}$<br>$-0.5(6279)(0.003)$<br>$f_f = 46.4\ ksi < f_{fu} = 62\ ksi \therefore$ Failure occurs indeed by concrete crushing. | $1.4\rho_{fb} = 0.0152$<br>Try using 6-No.6 bars with a cover of 1.5 inch and No. 3 stirrups:<br>$d = 16\ in. - 1.5 - 0.375 - (0.743/2) = 13.75\ in.$<br>$A_f = 0.433\ in.^2 (6) = 2.60\ in.^2$<br>$\rho_f = \frac{A_f}{bd}$<br>$\rho_f = \frac{2.60\ in.^2}{10.5\ in.(13.75\ in.)} = 0.0180 > 1.4\rho_{fb} \therefore \phi = 0.7$<br><br>Find the FRP bar stress when the ultimate strain of 0.003 in the concrete is reached:<br>$f_f = \sqrt{\frac{(E_f \varepsilon_{cu})^2}{4} + \frac{0.85\beta_1 f_c'}{\rho_f} E_f \varepsilon_{cu}} - 0.5 E_f \varepsilon_{cu} \le f_{fu}$<br>$f_f = \sqrt{\frac{[6279(0.003)]^2}{4} + \frac{0.85(0.85)(4)}{0.0180}(6279)(0.003)}$<br>$-0.5(6279)(0.003)$<br>$f_f = 46.4\ ksi < f_{fu} = 62\ ksi \therefore$ Failure occurs indeed by concrete crushing. |

**Figure 2: Design Example. (Continued)**

| Design based on ACI 440.1R-03 design guidelines | Design based on results from this research project |
|---|---|
| Nominal Moment capacity:<br>$M_n = \rho_f f_f \left(1 - 0.59 \frac{\rho_f f_f}{f_c'}\right) bd^2$<br>$M_n = (0.0180)(46.4)\left[1 - 0.59\frac{(0.0180)(46.4)}{4}\right](10)(13.75)^2$<br>$M_n = 1385\ kip \cdot in. = 115.4\ kip \cdot ft$<br><br>Provided moment capacity:<br>$\phi M_n \geq M_u$<br>$\phi M_n = (0.7)115.2\ kip \cdot ft = 80.8\ kip \cdot ft$<br>$\phi M_n = 80.8\ kip \cdot ft \geq M_u = 76.6\ kip \cdot ft \therefore$ The section has adequate flexural strength.<br><br>Minimum reinforcement:<br>$A_{f,\min} = \frac{5.4\sqrt{f_c'}}{f_{fu}} b_w d$<br>The minimum reinforcement requirement does not need to be checked because the section is over-reinforced. | Nominal Moment capacity:<br>$M_n = \rho_f f_f \left(1 - 0.59 \frac{\rho_f f_f}{f_c'}\right) bd^2$<br>$M_n = (0.0180)(46.4)\left[1 - 0.59\frac{(0.0180)(46.4)}{4}\right](10)(13.75)^2$<br>$M_n = 1385\ kip \cdot in. = 115.4\ kip \cdot ft$<br><br>Provided moment capacity:<br>$\phi M_n \geq M_u$<br>$\phi M_n = (0.7)115.2\ kip \cdot ft = 80.8\ kip \cdot ft$<br>$\phi M_n = 80.8\ kip \cdot ft \geq M_u = 76.6\ kip \cdot ft \therefore$ The section has adequate flexural strength.<br><br>Minimum reinforcement:<br>$A_{f,\min} = \frac{5.4\sqrt{f_c'}}{f_{fu}} b_w d$<br>The minimum reinforcement requirement does not need to be checked because the section is over-reinforced. |

**Figure 2: Design Example. (Continued)**

| Design based on ACI 440.1R-03 design guidelines | Design based on results from this research project |
|---|---|
| **5. Check the short-and long-term deflections of the beam,**<br><br>*Short-term deflection*<br>Gross moment of inertia of the beam:<br>$I_g = \frac{bh^3}{12}$<br>$I_g = \frac{(10.5\ in.)(16\ in.)^3}{12} = 3584\ in.^3$<br>Modular ratio:<br>$n_f = \frac{E_f}{E_c} = \frac{E_f}{57000\sqrt{f_c'}}$<br>$n_f = \frac{6279000\ psi}{57000\sqrt{4000\ psi}} = 1.74$<br><br>Neutral axis depth:<br>$k = \sqrt{2\rho_f n_f + (\rho_f n_f)^2} - \rho_f n_f$<br>$k = \sqrt{2(0.0180)(1.74) + [(0.0180)(1.74)]^2} - (0.0180)(1.74)$<br>$k = 0.221$<br><br>$I_{cr} = \frac{bd^3}{3}k^3 + n_f A_f d^2 (1-k)^2$ | **5. Check the short-and long-term deflections of the beam,**<br><br>*Short-term deflection*<br>Gross moment of inertia of the beam:<br>$I_g = \frac{bh^3}{12}$<br>$I_g = \frac{(10.5\ in.)(16\ in.)^3}{12} = 3584\ in.^3$<br>Modular ratio:<br>$n_f = \frac{E_f}{E_c} = \frac{E_f}{57000\sqrt{f_c'}}$<br>$n_f = \frac{6279000\ psi}{57000\sqrt{4000\ psi}} = 1.74$<br><br>Neutral axis depth:<br>$k = \sqrt{2\rho_f n_f + (\rho_f n_f)^2} - \rho_f n_f$<br>$k = \sqrt{2(0.0180)(1.74) + [(0.0180)(1.74)]^2} - (0.0180)(1.74)$<br>$k = 0.221$<br><br>$I_{cr} = \frac{bd^3}{3}k^3 + n_f A_f d^2 (1-k)^2$ |

**Figure 2: Design Example. (Continued)**

| Design based on ACI 440.1R-03 design guidelines | Design based on results from this research project |
|---|---|
| $I_{cr} = \frac{(10)(13.75)^3}{3}(0.221)^3 + 1.74(2.60)(13.75)^2(1-0.221)^2$<br>$I_{cr} = 613\ in.^4$<br>Compute the reduction coefficient for deflections using $\alpha_b$ = 0.50 for FRP bars having the same bond strength as steel bars:<br>$\beta_d = \alpha_b\left(\frac{E_f}{E_s}+1\right)$<br>$\beta_d = 0.50\left(\frac{6279\ ksi}{29000\ ksi}+1\right) = 0.608$<br><br>Moment due to dead load plus live load:<br>$M_{DL+LL} = \frac{w_{DL+LL}\cdot l^2}{8}$<br>$M_{DL+LL} = \frac{\left(0.775\frac{kip}{ft}+1.2\frac{kip}{ft}\right)(14\ ft)^2}{8} = 48.4\ kip\cdot ft$<br><br>Cracking moment:<br>$M_{cr} = \frac{f_r I_g}{y_t} = \frac{7.5\sqrt{f_c'}I_g}{\frac{h}{2}}$ | $I_{cr} = \frac{(10)(13.75)^3}{3}(0.221)^3 + 1.74(2.60)(13.75)^2(1-0.221)^2$<br>$I_{cr} = 613\ in.^4$<br>Compute the reduction coefficient for deflections using $\alpha_b$ = 0.50 for FRP bars having the same bond strength as steel bars:<br>$\beta_d = \alpha_b\left(\frac{E_f}{E_s}+1\right)$<br>$\beta_d = 0.50\left(\frac{6279\ ksi}{29000\ ksi}+1\right) = 0.608$<br><br>Moment due to dead load plus live load:<br>$M_{DL+LL} = \frac{w_{DL+LL}\cdot l^2}{8}$<br>$M_{DL+LL} = \frac{\left(0.775\frac{kip}{ft}+1.2\frac{kip}{ft}\right)(14\ ft)^2}{8} = 48.4\ kip\cdot ft$<br><br>Cracking moment:<br>$M_{cr} = \frac{f_r I_g}{y_t} = \frac{7.5\sqrt{f_c'}I_g}{\frac{h}{2}}$ |

**Figure 2: Design Example. (Continued)**

| Design based on ACI 440.1R-03 design guidelines | Design based on results from this research project |
|---|---|
| $M_{cr} = \frac{7.5\sqrt{4000\ psi}\left(3584\ in.^4\right)}{\frac{16\ in.}{2}}\left(\frac{1\ kip}{1000\ lb}\right)\left(\frac{1\ ft}{12\ in.}\right) = 17.7\ kip \cdot ft$ | $M_{cr} = \frac{7.5\sqrt{4000\ psi}\left(3584\ in.^4\right)}{\frac{16\ in.}{2}}\left(\frac{1\ kip}{1000\ lb}\right)\left(\frac{1\ ft}{12\ in.}\right) = 17.7\ kip \cdot ft$ |
| Cracked moment of inertia: | Cracked moment of inertia: |
| $(I_e)_{DL+LL} = \left(\frac{M_{cr}}{M_{DL+LL}}\right)^3 \beta_d I_g + \left[1 - \left(\frac{M_{cr}}{M_{DL+LL}}\right)^3\right] I_{cr}$ | $(I_e)_{DL+LL} = \left(\frac{M_{cr}}{M_{DL+LL}}\right)^3 \beta_d I_g + \left[1 - \left(\frac{M_{cr}}{M_{DL+LL}}\right)^3\right] I_{cr}$ |
| $(I_e)_{DL+LL} = \left(\frac{17.7}{48.4}\right)^3 (0.608)(3584) + \left[1 - \left(\frac{17.7}{48.4}\right)^3\right](613)$ | $(I_e)_{DL+LL} = \left(\frac{17.7}{48.4}\right)^3 (0.608)(3584) + \left[1 - \left(\frac{17.7}{48.4}\right)^3\right](613)$ |
| $(I_e)_{DL+LL} = 690\ in.^4$ | $(I_e)_{DL+LL} = 690\ in.^4$ |
| Midspan deflection due to dead and live load: | Midspan deflection due to dead and live load: |
| $(y_i)_{DL+LL} = \frac{5 w_{DL+LL} \cdot l^4}{384 E_c (I_e)_{DL+LL}}$ | $(y_i)_{DL+LL} = \frac{5 w_{DL+LL} \cdot l^4}{384 E_c (I_e)_{DL+LL}}$ |
| $(y_i)_{DL+LL} = \frac{5\left(0.775\frac{kip}{ft} + 1.2\frac{kip}{ft}\right)(14\ ft)^4 \left(12\frac{in.}{ft}\right)^3}{384\left(3605\ ksi\right)\left(695\ in.^4\right)} = 0.69\ in.$ | $(y_i)_{DL+LL} = \frac{5\left(0.775\frac{kip}{ft} + 1.2\frac{kip}{ft}\right)(14\ ft)^4 \left(12\frac{in.}{ft}\right)^3}{384\left(3605\ ksi\right)\left(695\ in.^4\right)} = 0.69\ in.$ |
| Midspan deflections due to dead load alone and live load alone: | Midspan deflections due to dead load alone and live load alone: |
| $(y_i)_{DL} = \frac{w_{DL}}{w_{DL+LL}}(y_i)_{DL+LL}$ | $(y_i)_{DL} = \frac{w_{DL}}{w_{DL+LL}}(y_i)_{DL+LL}$ |

**Figure 2: Design Example. (Continued)**

| Design based on ACI 440.1R-03 design guidelines | Design based on results from this research project |
|---|---|
| $(y_i)_{DL} = \frac{0.775\frac{kip}{ft}}{0.775\frac{kip}{ft}+1.2\frac{kip}{ft}}(0.69\ in.) = 0.27\ in.$<br><br>$(y_i)_{LL} = \frac{w_{LL}}{w_{DL+LL}}(y_i)_{DL+LL}$<br><br>$(y_i)_{LL} = \frac{1.2\frac{kip}{ft}}{0.775\frac{kip}{ft}+1.2\frac{kip}{ft}}(0.69\ in.) = 0.42\ in.$<br><br>Allowable instantaneous live load deflection:<br><br>$(y_i)_{LL} = \frac{l}{360}$<br><br>$0.42\ in. < \frac{(14\ ft)\left(12\frac{in}{ft}\right)}{360} = 0.47\ in. \therefore$ O.K.<br><br>*Long-term deflection:*<br>$\xi = 1.25$ (ACI 318 for a duration of six months)<br>$\lambda = 0.60\xi$<br>$\lambda = 0.60(1.25) = 0.75$<br><br>Compute six-month deflection and compare to allowable:<br>$y_{LT} = (y_i)_{LL} + \lambda(y_i)_{DL}$<br>$y_{LT} = (0.42\ in.) + 0.75(0.27\ in.) = 0.62\ in.$ | $(y_i)_{DL} = \frac{0.775\frac{kip}{ft}}{0.775\frac{kip}{ft}+1.2\frac{kip}{ft}}(0.69\ in.) = 0.27\ in.$<br><br>$(y_i)_{LL} = \frac{w_{LL}}{w_{DL+LL}}(y_i)_{DL+LL}$<br><br>$(y_i)_{LL} = \frac{1.2\frac{kip}{ft}}{0.775\frac{kip}{ft}+1.2\frac{kip}{ft}}(0.69\ in.) = 0.42\ in.$<br><br>Allowable instantaneous live load deflection:<br><br>$(y_i)_{LL} = \frac{l}{360}$<br><br>$0.42\ in. < \frac{(14\ ft)\left(12\frac{in}{ft}\right)}{360} = 0.47\ in. \therefore$ O.K.<br><br>*Long-term deflection due to dead load:*<br><br>Compute initial top fiber strain and curvature at midspan.<br><br>Area of transformed section in compression:<br>$A_c = bkd = (10.5\ in.)(0.221)(13.75\ in.) = 31.9\ in.^2$<br><br>First moment of area of transformed section in compression about top surface:<br>$B_c = b\frac{(kd)^2}{2} = (10.5\ in.)\frac{\left[(0.221)(13.75\ in.)\right]^2}{2} = 48.5\ in.^3$ |

**Figure 2: Design Example. (Continued)**

| Design based on ACI 440.1R-03 design guidelines | Design based on results from this research project |
|---|---|
| Allowable long-term deflection:<br>$y_{LT} \le \frac{l}{240}$<br>$0.62\ in. < \frac{(14\ ft)\left(12\ \frac{in.}{ft}\right)}{240} = 0.70\ in. \therefore$ OK | Moment of inertia of transformed section in compression about top surface:<br>$I_c = b\frac{(kd)^3}{12} + b\frac{(kd)^2}{2}$<br>$I_c = (10.5\ in.)\frac{\left[(0.221)(13.75\ in.)\right]^3}{12} + (10.5\ in.)\frac{\left[(0.221)(13.75\ in.)\right]^3}{4}$<br>$I_c = 98.3\ in.^4$<br>$A_c^{'} = A_c + \frac{B_c - dA_c}{d\left(1-\frac{k}{3}\right)}$<br>$A_c^{'} = 31.9\ in.^2 + \frac{48.5\ in.^3 - (13.75\ in.)(31.9\ in.^2)}{13.75\ in.\left(1-\frac{0.221}{3}\right)} = 1.27\ in.^2$<br>$B_c^{'} = B_c + \frac{I_c - dB_c}{d\left(1-\frac{k}{3}\right)}$<br>$B_c^{'} = 48.5\ in.^3 + \frac{98.3\ in.^4 - (13.75\ in.)(48.5\ in.^3)}{13.75\ in.\left(1-\frac{0.221}{3}\right)} = 3.86\ in.^3$<br>Moment due to dead load:<br>$M_{DL} = \frac{w_{DL} \cdot l^2}{8}$ |

**Figure 2: Design Example. (Continued)**

| Design based on ACI 440.1R-03 design guidelines | Design based on results from this research project |
|---|---|
| | $M_{DL} = \frac{\left(0.775 \frac{kip}{ft}\right)\left(14\ ft\right)^2}{8} = 19.0\ kip \cdot ft$<br>Initial top fiber strain and curvature at midspan:<br>$\varepsilon_{oiC} = \frac{19\ kip \cdot ft\left(\frac{12\ in.}{1\ ft}\right)\left(3.86\ in.^3\right)}{3605\ ksi\left[\left(48.5\ in.^3\right)^2 - \left(98.3 in.^4\right)\left(31.9 in.^2\right)\right]} = -3.12x10^{-4}\ in./in.$<br>$\kappa_{iC} = \frac{-\left(1.27\ in.^2\right)\left(19\ kip \cdot ft\right)\left(\frac{12\ in.}{1\ ft}\right)}{3605\ ksi\left[\left(48.5 in.^3\right)^2 - \left(98.3 in.^4\right)\left(31.9 in.^2\right)\right]} = 1.02x10^{-4} in.^{-1}$<br>Check curvature:<br>$\kappa_{iC} = \frac{M_i}{E_c I_{cr}} = \frac{19\ kip \cdot ft\left(\frac{12\ in.}{1\ ft}\right)}{\left(3605\ ksi\right)\left(613\ in.^4\right)} = 1.03x10^{-4} in.^{-1} \quad \therefore \text{OK}$<br>Check top fiber strain:<br>$\varepsilon_{oiC} = -k_{ic} kd = -\left(1.02x10^{-4} in^{-1}\right)\left(0.221\right)\left(13.75\ in.\right)$<br>$\varepsilon_{oiC} = -3.10x10^{-4} in./in. \therefore \text{OK}$<br>Creep coefficient at six months:<br>Assume $C_{ult}$ = 2.35.<br>$\Delta\phi(t,\tau) = \frac{\left(t-\tau\right)^{0.6}}{D + \left(t-\tau\right)^{0.6}} C_{ult}$ |

**Figure 2: Design Example. (Continued)**

| Design based on ACI 440.1R-03 design guidelines | Design based on results from this research project |
|---|---|
| | $\Delta\phi(180,14) = \frac{(180-14)^{0.6}}{10+(180-14)^{0.6}}(2.35) = 1.60$<br>Choose an aging coefficient $\chi$ = 0.8, as recommended by Gilbert and Mickleborough:<br><br>Shrinkage strain at six months:<br>Assume the beam was cured for 7 days.<br>$(\varepsilon_{sh})_t = \frac{t}{35+t}(\varepsilon_{sh})_{ult}$<br>Assume $(\varepsilon_{sh})_{ult}$ = -730$x10^{-6}$<br>$(\varepsilon_{sh})_{180-7} = \frac{(180-7)}{35+(180-7)}(-730x10^{-6}) = -6.07x10^{-4}\, in./in.$<br><br>Obtain an equivalent imaginary creep loss of prestressing force at six months.<br><br>As explained in the creep test results section, the creep strain can be assumed to be independent of stress. Thus, for a beam with a distributed load, the creep strain will be assumed to be constant over the full length of the 14-ft span.<br><br>The creep strain at six months of 234$x10^{-6}$ inch/inch from specimen V1-5-b of the creep test will be used. |

**Figure 2: Design Example. (Continued)**

| Design based on ACI 440.1R-03 design guidelines | Design based on results from this research project |
|---|---|
| | Thus, the equivalent imaginary creep loss of prestressing force is:<br>$F = \Delta P = -\varepsilon_{c1} E_f A_f = -234x10^{-6}\ \frac{in.}{in.}\left(6279\ ksi\right)\left(2.60\ in.^2\right) = -3.82\ kip$<br>Age-adjusted effective modulus:<br>$E_e(t,\tau) = \frac{E_c}{1+\chi\Delta\phi(t,\tau)}$<br>$E_e(t,\tau) = \frac{3605\ ksi}{1+(0.8)(1.60)} = 1591\ ksi$<br><br>Total restraining forces at midspan:<br>$-\delta N = -E_e\left[\Delta\phi\left(A_c\varepsilon_{oiC} + B_c\kappa_{iC}\right) + \varepsilon_{sh}A_c\right] + \sum_{j=1}^{m} F_j$<br>$A_c\varepsilon_{oiC} + B_c\kappa_{iC} = \left(31.9\ in.^2\right)\left(-3.12x10^{-4}\right) + \left(48.5\ in.^3\right)\left(1.02x10^{-4}\ in.^{-1}\right)$<br>$A_c\varepsilon_{oiC} + B_c\kappa_{iC} = -5.0x10^{-3}\ in.^2$<br>$\Delta\phi\left(A_c\varepsilon_{oiC} + B_c\kappa_{iC}\right) + \varepsilon_{sh}A_c = 1.6\left(-5.0x10^{-3}\ in.^2\right) + \left(-6.07x10^{-4}\right)\left(31.9\ in.^2\right)$<br>$\Delta\phi\left(A_c\varepsilon_{oiC} + B_c\kappa_{iC}\right) + \varepsilon_{sh}A_c = -0.0273\ in.^2$<br>$-\delta N = -1579\ ksi\left(-0.0273\ in.^2\right) - 3.82\ kip$<br>$-\delta N = 39.3\ kip$ |

**Figure 2: Design Example. (Continued)**

| Design based on ACI 440.1R-03 design guidelines | Design based on results from this research project |
|---|---|
| | $-\delta M = -E_e\left[\Delta\phi\left(B_c\varepsilon_{oi} + I_c\kappa_i\right) + \varepsilon_{sh}B_c\right] + \sum_{j=1}^{m} F_j d_j$<br>$B_c\varepsilon_{oiC} + I_c\kappa_{iC} = \left(48.5\ in.^3\right)\left(-3.12x10^{-4}\right) + \left(98.3\ in.^4\right)\left(1.02x10^{-4}\ in.^{-1}\right)$<br>$B_c\varepsilon_{oiC} + I_c\kappa_{iC} = -5.11x10^{-3}\ in.^3$<br>$\Delta\phi\left(B_c\varepsilon_{oiC} + I_c\kappa_{iC}\right) + \varepsilon_{sh}B_c = 1.6\left(-5.11x10^{-3}\ in.^3\right) + \left(-6.07x10^{-4}\right)\left(48.5\ in.^3\right)$<br>$\Delta\phi\left(B_c\varepsilon_{oiC} + I_c\kappa_{iC}\right) + \varepsilon_{sh}B_c = -0.0376\ in.^3$<br>$Fd = \left(-3.82\ kip\right)\left(13.75\ in.\right)\left(\frac{1\ ft}{12\ in.}\right) = -4.38\ kip \cdot ft$<br>$-\delta M = -1579\ ksi\left(-0.0376\ in.^3\right)\left(\frac{1\ ft}{12\ in.}\right) - 4.38\ kip \cdot ft$<br>$-\delta M = 0.57\ kip \cdot ft$<br><br>Properties of age-adjusted transformed section:<br><br>Area of age-adjusted transformed section:<br>$A_e = bkd + n_{fe}A_f$<br>$n_{fe} = \frac{E_f}{E_e} = \frac{6279\ ksi}{1579\ ksi} = 3.98$<br>$A_e = \left(10.5\ in.\right)\left(0.221\right)\left(13.75\ in.\right) + 3.98\left(2.6\ in.^2\right) = 42.2\ in.^2$ |

**Figure 2: Design Example. (Continued)**

| Design based on ACI 440.1R-03 design guidelines | Design based on results from this research project |
|---|---|
| | First moment of area of age-adjusted transformed section about top of surface:<br>$B_e = b\frac{(kd)^2}{2} + n_{fe}A_f d$<br>$B_e = (10.5\ in.)\frac{\left[(0.221)(13.75\ in.)\right]^2}{2} + 3.98\left(2.6\ in.^2\right)(13.75\ in.) = 191\ in.^3$<br>Moment of inertia of transformed section in compression about top of surface:<br>$I_e = b\frac{(kd)^3}{12} + b\frac{(kd)^2}{2} + n_{fe}A_f d^2$<br>$I_e = (10.5\ in.)\frac{\left[(0.221)(13.75\ in.)\right]^3}{12} + (10.5\ in.)\frac{\left[(0.221)(13.75\ in.)\right]^3}{4}$<br>$+3.98\left(2.6\ in.^2\right)(13.75\ in.)^2$<br>$I_e = 2054\ in.^4$<br>$A_e^{'} = A_e + \frac{B_e - dA_e}{d\left(1-\frac{k}{3}\right)}$<br>$A_e^{'} = 42.2\ in.^2 + \frac{191\ in.^3 - (13.75\ in.)\left(42.2\ in.^2\right)}{13.75\ in.\left(1-\frac{0.221}{3}\right)} = 11.6\ in.^2$ |

**Figure 2: Design Example. (Continued)**

| Design based on ACI 440.1R-03 design guidelines | Design based on results from this research project |
|---|---|
| | $B_e^{'} = B_e + \frac{I_e - dB_e}{d\left(1-\frac{k}{3}\right)}$<br><br>$B_e^{'} = 191\ in.^3 + \frac{2054\ in.^4 - (13.75\ in.)(191\ in.^3)}{13.75\ in.\left(1-\frac{0.221}{3}\right)} = 146\ in.^3$<br><br>Time-dependent increments of curvature and top surface strain at midspan:<br>$\Delta\varepsilon_{oC} = \frac{\delta M B_e^{'} - \delta N I_e}{E_e\left(B_e^2 - I_e A_e\right)}$<br><br>$\Delta\varepsilon_{oC} = \frac{(-0.57\ kip\cdot ft)\left(\frac{12\ in.}{1\ ft}\right)(146\ in.^3) - (-39.4\ kip)(2054\ in.^4)}{1579\ ksi\left[(191\ in.^3)^2 - (2054\ in.^4)(42.2\ in.^2)\right]}$<br><br>$\Delta\varepsilon_{oC} = -1.01x10^{-3}$<br><br>$\Delta\kappa_C = \frac{B_e\delta N - A_e^{'}\delta M}{E_e\left(B_e^2 - I_e A_e\right)}$<br><br>$\Delta\kappa_C = \frac{(191\ in.^3)(-39.4\ kip) - (11.6\ in.^2)(-0.57\ kip\cdot ft)\left(\frac{12\ in.}{1\ ft}\right)}{1579\ ksi\left[(191\ in.^3)^2 - (2054\ in.^4)(42.2\ in.^2)\right]}$<br><br>$\Delta\kappa_C = 9.39x10^{-5}\ in.^{-1}$<br>$\varepsilon_{oC} = \varepsilon_{oiC} + \Delta\varepsilon_{oC} = -1.31x10^{-3}\ in./in.$ |

**Figure 2: Design Example. (Continued)**

| Design based on ACI 440.1R-03 design guidelines | Design based on results from this research project |
|---|---|
| | Final curvature and top surface strain at midspan:<br>$\kappa_C = \kappa_{iC} + \Delta\kappa = 1.96x10^{-4}\, in.^{-1}$<br>Initial top fiber strain and curvature at left support:<br>$\varepsilon_{oiL} = \frac{M_i B_c^{'} - N_i I_c}{E_c\left(B_c^2 - I_c A_c\right)} = 0$ since $Mi=0$ and $Ni=0$<br>$\kappa_{iL} = \frac{B_c N_i - A_c^{'} M_i}{E_c\left(B_c^2 - I_c A_c\right)} = 0$ since $Mi=0$ and $Ni=0$<br>Total restraining forces at left support:<br>$-\delta N = -E_e\left[\Delta\phi\left(A_c\varepsilon_{oiL} + B_c\kappa_{iL}\right) + \varepsilon_{sh}A_c\right] + \sum_{j=1}^{m} F_j$<br>$-\delta N = -E_e\left(\varepsilon_{sh}A_c\right) + \sum_{j=1}^{m} F_j$<br>$-\delta N = -1579\ ksi\left[\left(-6.07x10^{-4}\right)\left(31.9\, in.^2\right)\right] - 3.82\ kip = 26.8\ kip$<br>$-\delta M = -E_e\left[\Delta\phi\left(B_c\varepsilon_{oiL} + I_c\kappa_{iL}\right) + \varepsilon_{sh}B_c\right] + \sum_{j=1}^{m} F_j d_j$<br>$-\delta M = -E_e\left(\varepsilon_{sh}B_c\right) + \sum_{j=1}^{m} F_j d_j$<br>$-\delta M = -1579\ ksi\left[\left(-6.07x10^{-4}\right)\left(48.5\, in.^3\right)\right]\left(\frac{1\ ft}{12\ in.}\right) - 4.38\ kip\cdot ft$<br>$-\delta M = -0.50\ kip\cdot ft$ |

**Figure 2: Design Example. (Continued)**

| Design based on ACI 440.1R-03 design guidelines | Design based on results from this research project |
|---|---|
| | Time-dependent increments of curvature and top surface strain:<br>$\Delta\varepsilon_{oL} = \frac{\delta M B_e^{'} - \delta N I_e}{E_e\left(B_e^2 - I_e A_e\right)}$<br>$\Delta\varepsilon_{oL} = \frac{\left(0.50\ kip\cdot ft\right)\left(\frac{12\ in.}{1\ ft}\right)\left(146\ in.^3\right) - \left(-26.8\ kip\right)\left(2054\ in.^4\right)}{1579\ ksi\left[\left(191 in.^3\right)^2 - \left(2054\ in.^4\right)\left(42.2\ in.^2\right)\right]}$<br>$\Delta\varepsilon_{oL} = -7.02x10^{-4}$<br>$\Delta\kappa_L = \frac{B_e\delta N - A_e^{'}\delta M}{E_e\left(B_e^2 - I_e A_e\right)}$<br>$\Delta\kappa_L = \frac{\left(191\ in.^3\right)\left(-26.8\ kip\right) - \left(11.6\ in.^2\right)\left(0.50\ kip\cdot ft\right)\left(\frac{12\ in.}{1\ ft}\right)}{1579\ ksi\left[\left(191 in.^3\right)^2 - \left(2054\ in.^4\right)\left(42.2\ in.^2\right)\right]}$<br>$\Delta\kappa_L = 6.50x10^{-5}\ in.^{-1}$<br>Final curvature and top surface strain at left support:<br>$\varepsilon_{oL} = \varepsilon_{oiL} + \Delta\varepsilon_{oL} = -7.02x10^{-4}\ in./in.$<br>$\kappa_L = \kappa_{iL} + \Delta\kappa_L = 6.50x10^{-5}\ in.^{-1}$<br>Initial top fiber strain and curvature at right support:<br>$\varepsilon_{oiR} = 0\ ,\ \kappa_{iR} = 0$ |

**Figure 2: Design Example. (Continued)**

| Design based on ACI 440.1R-03 design guidelines | Design based on results from this research project |
|---|---|
| | Final curvature and top surface strain at left support:<br>$\varepsilon_{oR} = -7.02x10^{-4}\, in./in.$<br>$\kappa_R = 6.50x10^{-5}\, in.^{-1}$<br><br>Compute midspan deflection at six months due to dead load:<br>$(y_{LT})_{DL} = \frac{L^2}{96}(\kappa_L + 10\kappa_C + \kappa_R)$<br>$(y_{LT})_{DL} = \frac{\left[(14\ ft)\left(\frac{12\ in.}{1\ ft}\right)\right]^2}{96}\left(6.50x10^{-5}\, in.^{-1} + 10\left(1.02x10^{-4}\right) + 6.50x10^{-5}\, in.^{-1}\right)$<br>$(y_{LT})_{DL} = 0.61\ in.$<br><br>*Total six-month deflection at midspan:*<br>$y_{LT} = (y_i)_{LL} + (y_{LT})_{DL}$<br>$y_{LT} = 0.41\ in. + 0.61\ in. = 1.03\ in.$<br><br>Allowable long-term deflection:<br>$y_{LT} \le \frac{l}{240}$<br>$1.03\ in. > \frac{(14\ ft)\left(12\ \frac{in.}{ft}\right)}{240} = 0.70\ in. \therefore$ N.G.<br><br>Before redesigning the section, check the maximum crack width. |

**Figure 2: Design Example. (Continued)**

| Design based on ACI 440.1R-03 design guidelines | Design based on results from this research project |
|---|---|
| **6. Check the maximum crack width.**<br>Compute the stress level in the FRP bars under dead load plus live load (service conditions):<br>$f_f = \frac{M_{DL+LL}}{A_f d\left(1-\frac{k}{3}\right)}$<br>$f_f = \frac{48.4\ kip\cdot ft\left(\frac{12\ in.}{1\ ft}\right)}{\left(2.60\ in.^2\right)13.75\ in.\left(1-\frac{0.221}{3}\right)} = 17.5\ ksi$<br>Find the effective tension area of concrete:<br>$\beta = \frac{h-kd}{d-kd}$<br>$\beta = \frac{16\ in.-0.221\left(13.75\ in.\right)}{13.75\ in.-0.221\left(13.75\ in.\right)} = 1.21$<br>$d_c = cover + stirrup\ size + \frac{1}{2}d_b$<br>$d_c = 1.5\ in.+0.375+\frac{1}{2}\left(0.743\ in.\right) = 2.25\ in.$<br>$A = \frac{2\left(h-d\right)b}{No.\ bars}$<br>$A = \frac{2\left(16\ in.-13.75\ in.\right)\left(10.5\ in.\right)}{6} = 7.86\ in.^2$ | **6. Check the maximum crack width.**<br>Compute the stress level in the FRP bars under dead load plus live load (service conditions):<br>$f_f = \frac{M_{DL+LL}}{A_f d\left(1-\frac{k}{3}\right)}$<br>$f_f = \frac{48.4\ kip\cdot ft\left(\frac{12\ in.}{1\ ft}\right)}{\left(2.60\ in.^2\right)13.75\ in.\left(1-\frac{0.221}{3}\right)} = 17.5\ ksi$<br>Find the effective tension area of concrete:<br>$\beta = \frac{h-kd}{d-kd}$<br>$\beta = \frac{16\ in.-0.221\left(13.75\ in.\right)}{13.75\ in.-0.221\left(13.75\ in.\right)} = 1.21$<br>$d_c = cover + stirrup\ size + \frac{1}{2}d_b$<br>$d_c = 1.5\ in.+0.375+\frac{1}{2}\left(0.743\ in.\right) = 2.25\ in.$<br>$A = \frac{2\left(h-d\right)b}{No.\ bars}$<br>$A = \frac{2\left(16\ in.-13.75\ in.\right)\left(10.5\ in.\right)}{6} = 7.86\ in.^2$ |

**Figure 2: Design Example. (Continued)**

| Design based on ACI 440.1R-03 design guidelines | Design based on results from this research project |
|---|---|
| Compute the maximum crack width using ACI 440.1R-03 Equation 8-9b:<br>$w = 0.076\beta \frac{E_s}{E_f} f_f \sqrt[3]{d_c A}$<br>$w = 0.076(1.21)\frac{29000}{6279}(17.5\ ksi)\sqrt[3]{(2.25\ in.)(7.86\ in.^2)}$<br>$w = 19\ mils < 20\ mils \quad \therefore$ OK<br><br>Compute the maximum crack width using ACI 440.1R-03 Equation 8-9c, using the recommended value of $kb$ = 1.2:<br>$w = \frac{2200}{E_f}\beta k_b f_f \sqrt[3]{d_c A}$<br>$w = \frac{2200}{6279}(1.21)(1.2)(17.5\ ksi)\sqrt[3]{(2.25\ in.)(7.86\ in.^2)}$<br>$w = 23\ mils > 20\ mils \quad \therefore$ N.G. | Compute the maximum crack width using Equation 81 from this research:<br>$W_{\max} = 0.09\beta \cdot f_f \cdot \sqrt[3]{d_c A}$<br>$W_{max} = 0.09(1.21)\frac{29000}{6279}(17.5\ ksi)\sqrt[3]{(2.25\ in.)(7.86\ in.^2)}$<br>$W_{max} = 23\ mils > 20\ mils \quad \therefore$ N.G. Redesign the beam. |
| **5a. Check the short-and long-term deflections of the beam.**<br><br>The beam is adequate for short-term and long-term deflections. | **5a. Check the short-and long-term deflections of the beam.**<br><br>Try $h$ = 19 inches.<br>$\rho_f = \frac{A_f}{bd}$<br>$\rho_f = \frac{2.60\ in.^2}{10.5\ in.(16.75\ in.)} = 0.0148 < 1.4\rho_{fb} = 0.0152 \therefore \phi = 0.7$ |

**Figure 2: Design Example. (Continued)**

| Design based on ACI 440.1R-03 design guidelines | Design based on results from this research project |
|---|---|
| | Moment capacity:<br>$\phi M_n = 113.7\ kip \cdot ft \geq M_u = 77.7\ kip \cdot ft\ \therefore$ OK<br><br>Live load deflection:<br>$(y_i)_{LL} = 0.22\ in. < 0.47\ in.\ \therefore$ OK<br><br>Total long-term deflection:<br>$(y)_{LT} = 0.67\ in. \leq \frac{l}{240} = 0.70\ in.\ \therefore$ OK |
| **6a. Check the maximum crack width.**<br><br>The beam is adequate per ACI Equation 8-9b.<br><br>Try $h$ = 19 inches.<br><br>Compute the maximum crack width using ACI 440.1R-03 Equation 8-9c, using the recommended value of $kb$ = 1.2:<br>$w = 18.6\ mils < 20\ mils\ \therefore$ OK | **6a. Check the maximum crack width.**<br><br>Compute the maximum crack width using Equation 81 from this research:<br>$W_{max} = 18.4\ mils < 20\ mils\ \therefore$ OK |
| **7. Check the creep rupture stress limit.**<br><br>Moment due to sustained load:<br>$M_S = M_{DL}$<br>$M_S = \frac{0.808 \frac{kip}{ft} (14\ ft)^2}{8} = 19.8\ kip \cdot ft$ | **7. Check the creep rupture stress limit.**<br><br>Moment due to sustained load:<br>$M_S = M_{DL}$<br>$M_S = \frac{0.808 \frac{kip}{ft} (14\ ft)^2}{8} = 19.8\ kip \cdot ft$ |

**Figure 2: Design Example. (Continued)**

| Design based on ACI 440.1R-03 design guidelines | Design based on results from this research project |
|---|---|
| Sustained stress in the FRP bars:<br>$f_{f,S} = \frac{M_S}{A_f d\left(1-\frac{k}{3}\right)}$<br>$f_f = \frac{19.8\ kip\cdot ft\left(\frac{12\ in.}{1\ ft}\right)}{\left(2.6\ in.^2\right)16.75\ in.\left(1-\frac{0.203}{3}\right)} = 5.85\ ksi$<br>Check the stress limit for GFRP bars:<br>$f_{f,S} \le 0.20 f_{fu}$<br>$5.85\ ksi \le 0.20\left(62\ ksi\right) = 12.4\ ksi \quad \therefore$ O.K. | Sustained stress in the FRP bars:<br>$f_{f,S} = \frac{M_S}{A_f d\left(1-\frac{k}{3}\right)}$<br>$f_f = \frac{19.8\ kip\cdot ft\left(\frac{12\ in.}{1\ ft}\right)}{\left(2.6\ in.^2\right)16.75\ in.\left(1-\frac{0.203}{3}\right)} = 5.85\ ksi$<br>Check the stress limit for GFRP bars:<br>$f_{f,S} \le 0.20 f_{fu}$<br>$5.85\ ksi \le 0.20\left(62\ ksi\right) = 12.4\ ksi \quad \therefore$ O.K. |
| **8. Compute the basic development length.**<br>Use ACI Equation 11-7:<br>$l_{bf} = \frac{d_b f_{fu}}{2700} = \frac{\left(0.743\ in.\right)\left(62000\ psi\right)}{2700} = 17\ in.$ | **8. Compute the basic development length.**<br>Use Equation 90 from this research:<br>$l_{bf} = \frac{d_b f_{u,ave}}{2700} = \frac{\left(0.743\ in.\right)\left(96000\ psi\right)}{2700} = 26.4\ in.$ |
| **9. Compute additional deflections due to cyclic loading.**<br>ACI 440.1R-03 does not account for deflections due to cyclic loading. | **9. Compute additional deflections due to cyclic loading.**<br>Assume the cyclic loading will be due to live load alone. Thus, use the slope of Equation 84 from this research, and use the initial deflection due to dead load and live load. |



**Figure 2: Design Example. (Continued)**

| Design based on ACI 440.1R-03 design guidelines | Design based on results from this research project |
|---|---|
| | Initial deflection due to dead load and live load:<br>$(y_i)_{DL+LL} = \frac{5w_{DL+LL} \cdot l^4}{384E_c(I_e)_{DL+LL}}$<br>$(y_i)_{DL+LL} = \frac{5\left(0.808\ \frac{kip}{ft} + 1.2\ \frac{kip}{ft}\right)(14\ ft)^4\left(12\ \frac{in.}{ft}\right)^3}{384(3605\ ksi)(1299\ in.^4)} = 0.15\ in. + 0.22\ in.$<br>$(y_i)_{DL+LL} = 0.37\ in.$<br><br>Lower bound beam defection due to 2 million cycles of application of live load:<br>$y = 0.0046\ in.ln(n) + 0.37\ in.$<br>$y = 0.0046\ in.ln(2000000) + 0.37\ in. = 0.47\ in.$ |



**Figure 2: Design Example. (Continued)**

As a result of this review, the researchers proposed the following changes to the ACI 440.1R-03 design and construction guidelines. A reevaluation of the environmental reduction factors is proposed, since this research showed that they may not be conservative. Equation 2, presented earlier, is proposed to replace Equation 8, 9a in the ACI 440.1R-03 design and construction guide (2003). This research also proposes that the deflections of GFRP-reinforced concrete elements induced by cyclic loading also be accounted for in the ACI 440.1R-03 design and construction guidelines. Creep should be accounted for as shown in Report 9-1520-3 (Trejo et al. 2003). Equation 9 of this report is proposed to replace Equation 11-7 of the ACI 440.1R-03 design and construction guidelines. Finally, the minimum cover of 1 bar diameter recommended by the ACI 440.1R-03 design and construction guidelines cannot be verified for adequacy using this research. However, this research showed that a cover of 1.33 bar diameters has been shown by this research to have no cracking problems due to thermal expansion.

# III. PROPOSED REVISIONS TO THE AASHTO LRFD BRIDGE DESIGN SPECIFICATIONS

This section presents a review of the 1998 AASHTO LRFD bridge design specifications (1998) and recommends changes based on the results of this and other research related to the use of non-prestressed GFRP bars to reinforce concrete structures. This section presents a brief introduction followed by a description of the AASHTO sections that may need to be modified to include the design of concrete elements reinforced with FRP bars. The sections of the AASHTO specifications that do not need to be modified are not listed in this section.

The 1998 AASHTO LRFD bridge design specifications do not include recommendations for the design of concrete structures reinforced with GFRP bars. Because the results obtained by this research and by the studies referenced are limited to the conditions and exposures evaluated in this research, extreme care should be taken when designing GFRP-reinforced concrete elements that will be subjected to different conditions. It should be noted that these recommendations are proposed based on the research to date and in most cases more work is needed before implementing such modifications. A review of the applicable sections is presented next. Note that the section numbers listed below are the section numbers from the 1998 AASHTO LRFD bridge design specifications.

## PROPOSED REVISIONS

### 1. Add to Section 1.3.3 Ductility

This section of the code requires the bridge to develop significant and visible inelastic deformations at the strength and extreme event limit states. Since GFRP bars exhibit linearly elastic behavior up to failure, GFRP-reinforced concrete elements do not exhibit significant ductility. Naaman and Jeong (1995) indicated that although FRP-reinforced concrete beams may deform considerably before failure, they elastically store most of the energy imposed on them during loading. Thus, since inelastic deformations

are required by the code, either GFRP bars should not be used or GFRP bars should be used in combination with other systems or materials to provide ductility. Alternatively, the code may develop non-ductile behavior requirements for GFRP-reinforced concrete elements.

**2. Add to Section 2.5.2.1.1 Materials**

The degradation of GFRP reinforcement should be accounted for in design. The tensile strength of GFRP bars can degrade in the concrete. The durability of FRP-reinforced concrete structures can be affected by several environmental factors such as: acids, alkalis, high temperatures, ultraviolet radiation, organic solvents, and oxygen or ozone (Bakht et al. 2000). The bond strength between GFRP bars and concrete can degrade with time in high-temperature moist conditions.

**3. Add to Section 3.10.1 General**

The fact that FRP-reinforced concrete elements are non-ductile should be considered when performing a seismic design.

**4. Notice for Section 4.6.2 Approximate Methods of Analysis**

This section may require modifications because FRP-reinforced concrete elements with a given amount and distribution of reinforcement and a given geometry have lower stiffness than steel-reinforced concrete elements having the same geometry and amount and configuration of reinforcement.

**5. Notice for Section 5 Concrete Structures**

The ACI 440.1R-03 (2003) design and construction guidelines should be adopted for this section. However, special care must be taken to ensure that these equations and factors apply to the conditions at the actual structures' location because it has been determined that environmental conditions do affect the performance of GFRP reinforcing bars. Special consideration should be given to the subsections addressed in the following proposed revisions.

**6. Add to Section 5.4 Material Properties**

Consideration should be given in this section to the material properties of GFRP bars such as tensile strength, accounting for environmental reduction factors, as already discussed in the ACI 440.1R-03 design and construction guidelines, coefficient of thermal expansion of the FRP bars, creep of FRP bars, deflections due to cyclic loading, and deterioration of bond strength between GFRP bars and concrete. A description of the durability and reactivity of fibers and resins to different environmental conditions given in the Canadian Bridge Design code provisions for fiber-reinforced structures could be included in this section (Bakht et al. 2000). A summary of the deleterious effects of several environments on fibers and matrices as described by Bakht et al. (2000) is given next:

- *Water*: Polymeric fibers and matrices absorb moisture. Moisture absorption softens the polymers. There are not sufficient data for the rate of deterioration of carbon and glass fibers.
- *Weak acids*: Bridges in industrialized areas may be exposed to weak acids from acid rain and carbonization, with pH values between 4 and 7. Weak acids can attack glass fibers and polyester matrices.
- *Strong acids*: Accidental spillage may cause strong acids to come in contact with bridge components. Strong acids can attack glass fibers, aramid fibers, and polyester and epoxy matrices.
- *Weak alkalis*: Concrete containing pozzolans can have pH values between 7 and 10. Weak alkalis such as these materials can attack glass fibers and polyester matrices.
- *Strong alkalis*: Typical Portland cement concretes have pH values greater than 10 and can cause degradation of glass fibers. Strong alkalis can attack glass fibers, aramid fibers, and polyester matrices.
- *High temperatures*: Carbon and glass fibers are resistant to high temperatures. However, high temperatures adversely affect aramid fibers and polymeric matrices.

- *Ultraviolet radiation*: Carbon and glass fibers are resistant to ultraviolet radiation. However, ultraviolet radiation adversely affects aramid fibers and polymeric matrices.

**7. Move Section 5.4.4 Prestressing Steel to Section 5.4.5**

**8. Move Section 5.4.5 Posttensioning Anchorages and Couplers to Section 5.4.6**

**9. Move Section 5.4.6 Ducts to Section 5.4.7**

**10. Add Section 5.4.4 FRP Reinforcement**

**11. Add Section 5.4.4.1 General**

The design tensile strength of GFRP bars should be taken from the ACI 440.1R-03 design and construction guidelines as shown previously in Equation 1:

$$f_{fu} = C_E f_{fu}^*$$

**12. Add Section 5.4.4.2 Modulus of Elasticity**

The modulus of elasticity of FRP bars should be the average value reported from proper testing or by the manufacturer.

**13. Add to Section 5.5.3.2 Reinforcing Bars**

The results of the cyclic load tests conducted in this research indicate that the flexural strength of GFRP-reinforced concrete beams show no significant degradation after the application of 4 and 5 million cycles of an alternating load with a GFRP bar stress range of 18.9 ksi. The fatigue capacity of FRP bars to be used in a bridge should be validated by further tests.

**14. Add Section 5.5.4.2.4 FRP Construction**

The resistance factors recommended by the ACI 440.1R-03 design and construction guidelines should be used in this section. The resistance factors for flexure are:

$$\phi = 0.50 \text{ for } \rho_f \le \rho_{fb}$$

$$\phi = \frac{\rho_f}{2\rho_{fb}} \text{ for } \rho_f < \rho_{fb} < 1.4\rho_{fb} \qquad (12)$$

$$\phi = 0.70 \text{ for } \rho_f \ge 1.4\rho_{fb}$$

The resistance factor for shear should be the same as the factor used in the ACI 318 (2000) building code ($\phi = 0.85$).

**15. Add Section 5.7.3.2.5 FRP-Reinforced Concrete Elements**

The equations for flexural resistance given in the ACI 440.1R-03 design and construction guidelines should be used in this section. The reinforcement ratio ($\rho_f$) and the balanced reinforcement ratio ($\rho_{fb}$) for GFRP-reinforced sections can be computed with Equations 13 and 14, respectively:

$$\rho_f = \frac{A_f}{bd} \qquad (13)$$

$$\rho_{fb} = 0.85\beta_1 \frac{f_c'}{f_{fu}} \frac{E_f \varepsilon_{cu}}{E_f \varepsilon_{cu} + f_{fu}} \qquad (14)$$

where,

$A_f$ = Area of FRP reinforcement ($inch^2$),

$a$ = Depth of equivalent rectangular stress block ($inch$),

$b$ = Width of section ($inch$),

$d$ = Effective depth of the section ($inch$),

$\varepsilon_{cu}$ = Ultimate strain in concrete,

$\beta_1$ = Factor taken as 0.85 for values of f'$_c$ up to and including 4 ksi. Above 4 ksi, the factored is reduced linearly at a rate of 0.05 for each 1 ksi in excess of 4 ksi, but should not be smaller than 0.65,

$f_{fu}$ = Design tensile strength of FRP reinforcement (*ksi*),

$f'_c$ = Design compressive strength of concrete (*ksi*),

$E_f$ = Modulus of elasticity of FRP bars (*ksi*).

When the reinforcement ratio is below the balanced ratio, FRP rupture is the failure mode; otherwise, concrete crushing is the failure mode.

The ACI 440.1R-03 design and construction guidelines recommend the following equations to compute the nominal flexural capacity when the reinforcement ratio is greater than the balanced ratio:

$$M_n = A_f f_f \left( d - \frac{a}{2} \right) \tag{15}$$

$$a = \frac{A_f f_f}{0.85 f'_c b} \tag{16}$$

$$f_f = \left( \sqrt{\frac{\left(E_f \varepsilon_{cu}\right)^2}{4} + \frac{0.85 \beta_1 f'_c}{\rho_f} E_f \varepsilon_{cu}} - 0.5 E_f \varepsilon_{cu} \right) \leq f_{fu} \tag{17}$$

where,

$M_n$ = Nominal flexural capacity (*kip.inch*),

$f_f$ = Stress in the FRP reinforcement (*ksi*).

When the reinforcement ratio is smaller than the balanced ratio, the ACI 440.1R-03 design and construction guidelines recommend the following equation to compute the nominal flexural capacity:

$$M_n = 0.8 A_f f_{fu} \left( d - \frac{\beta_1 c_b}{2} \right) \tag{18}$$

$$c_b = \left( \frac{\varepsilon_{cu}}{\varepsilon_{cu} + \varepsilon_{fu}} \right) d \tag{19}$$

Where $\varepsilon_{fu}$ is the ultimate strain in the GFRP reinforcement and all other terms were previously defined.

**16. Add to Section 5.7.3.3.2 Minimum Reinforcement**

For FRP-reinforced concrete elements in which failure is controlled by FRP rupture, the minimum area of FRP reinforcement should be as recommended by the ACI 440.1R-03 design and construction guidelines:

$$A_{f,\min} = \frac{5.4\sqrt{f_c'}}{f_{fu}} b_w d \geq \frac{360}{f_{fu}} b_w d \qquad (20)$$

This requirement is intended to prevent flexural failure upon concrete cracking.

**17. Add to Section 5.7.3.4 Control of Cracking by Distribution of Reinforcement**

This section should use the allowable crack width for FRP-reinforced concrete elements as recommended by the ACI 440.1R-03 design and construction guidelines. The allowable maximum crack widths are 0.028 inches for interior exposure and 0.020 inches for exterior exposure.

Maximum crack widths can be estimated using the following equation, validated in this project and presented earlier as Equation 2:

$$W_{\max} = 0.09\beta \cdot f_f \cdot \sqrt[3]{d_c A}$$

**18. Add to Section 5.7.3.5 Moment Redistribution**

Following the ACI 440.1R-03 design and construction guidelines, since GFRP-reinforced concrete elements exhibit linear elastic behavior up to failure, moment redistribution should not be considered for GFRP-reinforced concrete.

**19. Add to Section 5.7.3.6.2 Deflection and Camber**

Deflection and camber of GFRP-reinforced concrete elements should consider GFRP creep. Equations 8-12a and 8-12b as recommended by the ACI 440.1R-03 design and construction guidelines to compute instantaneous deflections should be used:

$$I_e = \left(\frac{M_{cr}}{M_a}\right)^3 \beta I_g + \left[1 - \left(\frac{M_{cr}}{M_a}\right)^3\right] I_{cr} \leq I_g \qquad (21)$$

$$\beta = \alpha\left(\frac{E_f}{E_s} + 1\right) \tag{22}$$

where,

$I_{cr}$ = cracked moment of inertia of the section ($inch^4$),

$I_g$ = Gross moment of inertia of the section ($inch^4$),

and all other terms have been defined previously.

The long-term deflections can be computed using Equation 8-14, provided by the ACI 440.1R-03 design and construction guidelines and shown previously as Equation 6:

$$\Delta_{(cp+sh)} = 0.6\xi\left(\Delta_i\right)_{sus}$$

Alternatively, the change in curvature due to long-term loading can be computed using the following equation, shown earlier as Equation 7:

$$\Delta\kappa = \frac{B_e\delta N - A_e^{'}\delta M}{E_e\left(B_e^{\ 2} - A_e I_e\right)}$$

and the long-term deflections can be computed by substituting Equation 7 into Equation 8:

$$y_C = \frac{L^2}{96}\left(\kappa_A + 10\kappa_C + \kappa_B\right)$$

Cyclic loading of concrete beam tests shows that deflections due to cyclic loading can increase by 78 percent due to cyclic loading and should be included in the computation of deflections due to live load.

The slope of Equation 5 can be used to compute the lower bound deflection increments due to the application of cyclic load:

$$y = 0.0046\ln(n) + 0.0858$$

**20. Add to Section 5.8.2.5 Minimum Transverse Reinforcement**

The requirements for minimum transverse reinforcement provided by the ACI 440.1R-03 design and construction guidelines should be adopted in this section. The minimum transverse reinforcement for FRP-reinforced concrete sections is:

$$A_{fv,\min} = \frac{50 b_w s}{f_{fv}} \tag{23}$$

where,

$A_{fv,min}$ = Minimum area of transverse FRP reinforcement ($inch^2$),

$b_w$ = Width of section (*inch*),

$s$ = Spacing of stirrups (*inch*),

$f_{fv}$ = Stress level in the FRP shear reinforcement at ultimate (*ksi*).

According to the ACI 440.1R-03 design and construction guidelines, the stress level in the FRP shear reinforcement at ultimate should be limited to the following value to avoid failure at the bent portion of the FRP stirrup:

$$f_{fv} = 0.002 E_f \le f_{fb} \tag{24}$$

where $f_{fb}$ is the strength of a bent portion of an FRP stirrup (*ksi*).

**21. Add to Section 5.8.3.3 Nominal Shear Resistance**

The neutral axis depth of cracked FRP-reinforced concrete sections is smaller than that for steel-reinforced concrete elements due to the lower stiffness of FRP bars when compared to steel bars (ACI 2000). Thus, the contribution to shear strength by aggregate interlock, dowel action, and shear of compressed concrete are lower for FRP-reinforced concrete members than for steel-reinforced concrete members. This section should adopt the recommendations of the ACI 440.1R-03 design and construction guidelines for shear design of FRP-reinforced concrete members.

The ACI 440.1R-03 design and construction guide recommendations for the shear force taken by the concrete should be used:

$$V_{c,f} = \frac{\rho_f E_f}{90 \beta_1 f_c'} V_c \tag{25}$$

where the terms are as defined before and $V_c$ is the nominal shear force provided by the concrete for steel-reinforced concrete members as given in the ACI 318 code (2000). The value of $V_{c,f}$ should not be larger than $V_c$.

The required spacing and area of shear reinforcement when stirrups are used perpendicular to the member are:

$$\frac{A_{fv}}{s} = \frac{\left(V_u - \phi V_{c,f}\right)}{\phi \cdot f_{fv} d} \tag{26}$$

where the terms have been defined before and,

$A_{fv}$ = Area of shear reinforcement ($inch^2$),

$V_u$ = Factored shear force at section (*kips*).

**22. Add to Section 5.10.2.1 Standard Hooks**

The recommendation of ACI 440.1R-03 design and construction guidelines for a minimum tail length of 12 bar diameters should be used in this section.

**23. Add to Section 5.10.2.3 Minimum Bend Diameters**

The minimum ratio of radius of bend to bar diameter of three for FRP stirrups, as recommended by the ACI 440.1R-03 design and construction guidelines, should be considered in FRP-reinforced concrete elements.

**24. Add to Section 5.10.7 Transverse Reinforcement for Flexural Members**

A maximum spacing for transverse reinforcement of $d/2$ or 24 inches, as recommended by the ACI 440.1R-03 design and construction guidelines, should be considered in this section.

**25. Add to Section 5.10.8 Shrinkage and Temperature Reinforcement**

The ACI 440.1R-03 design and construction guidelines recommended minimum reinforcement ratio for temperature and shrinkage $\rho_{f,ts}$ should be used in this section (but need not be more than 0.00036):

$$\rho_{f,ts} = 0.0018\frac{60{,}000}{f_{fu}}\frac{E_s}{E_f} \geq 0.0014 \qquad (27)$$

**26. Notice for Section 5.10.11 Provisions for Seismic Design**

Since GFRP reinforcement is non-ductile, provisions should be taken in the design of GFRP-reinforced concrete elements where ductility is required.

**27. Add to Section 5.11.2.1.1 Tension Development Length**

This research recommends that the basic development length of GFRP-reinforced concrete elements be computed with the following equation, shown earlier as Equation 11:

$$l_{bf} = \frac{d_b f_{u,ave}}{2700}$$

**28. Add to Section 5.11.2.1.2 Modification Factors that Increase $l_d$**

The ACI 440.1R-03 design and construction guidelines recommend a modification factor of 1.3 for top bars to obtain the development length of an FRP bar ($l_{df}$).

**29. Add to Section 5.11.2.4.1 Basic Hook Development Length**

The recommended development length for a bent bar provided by the ACI 440.1R-03 design and construction guidelines should be used in this section. The development length for hooked bars is determined as follows:

$$l_{bhf} = 2000\frac{d_b}{\sqrt{f_c'}} \cdot for \cdot f_{fu} \leq 75{,}000\ psi$$

$$l_{bhf} = \frac{f_{fu}}{37.5}\frac{d_b}{\sqrt{f_c'}} \cdot for \cdot 75{,}000\ psi < f_{fu} < 150{,}000\ psi \qquad (28)$$

$$l_{bhf} = 4000\frac{d_b}{\sqrt{f_c'}} \cdot for \cdot f_{fu} \geq 150{,}000\ psi$$

The development length computed with Equation 28 should not be less than 12 $d_b$ or 9 inches.

**30. Add to Section 5.11.5.3.1 Lap Splices in Tension**

There is limited research in this area. However, the ACI 440.1R-03 design and construction guidelines recommend using values of 1.3 $l_{df}$ for class A and 1.6 $l_{df}$ for class C splices (as defined by AASHTO). Since the value of 1.7 $l_d$ for class C splice recommended by AASHTO is more conservative, it is advisable to use that value to compute the development length of spliced FRP bars.

**31. Add to Section 5.12 Durability**

This section should give special consideration to the durability of GFRP reinforcement. Refer to the new proposed section 5.4 Material Properties (recommended by this research to be added to the AASHTO LRFD specifications) for a brief description of environmental effects on GFRP bars. A summary of the deleterious effects of several environments on fibers and matrices as described previously is repeated next:

- *Water*: Moisture absorption softens the polymers. There are not sufficient data for the rate of deterioration of carbon and glass fibers.
- *Weak acids*: Weak acids can attack glass fibers and polyester matrices.
- *Strong acids*: Strong acids can attack glass fibers, aramid fibers, and polyester and epoxy matrices.
- *Weak alkalis*: Weak alkalis can attack glass fibers and polyester matrices.
- *Strong alkalis*: Strong alkalis can attack glass fibers, aramid fibers, and polyester matrices.
- *High temperatures*: Carbon and glass fibers are resistant to high temperatures. Nevertheless, high temperatures adversely affect aramid fibers and polymeric matrices.

- *Ultraviolet radiation*: Carbon and glass fibers are resistant to ultraviolet radiation. However, ultraviolet radiation adversely affects aramid fibers and polymeric matrices.

**32. Add to Section 5.12.3 Concrete Cover**

This section of the code specifies a minimum cover for exterior exposure of 2 inches. The recommended covers should consider the fact that a 1-inch cover for a concrete deck with compressive strength of approximately 5.88 ksi and a 0.75-inch diameter bar does not cause cracking due to thermal expansion. This implies that, according to this research, a cover of 1.33 bar diameters is adequate to avoid cracking due to thermal expansion for typical conditions encountered by bridge superstructures. The 2-inch cover should be adequate for elements reinforced with 0.75-inch and smaller diameter bars. The cover depth design of elements exposed to direct solar radiation reinforced with bar diameters larger than 0.75 inch should be supported by tests.

# IV. RECOMMENDED CONSTRUCTION GUIDELINES FOR THE USE OF GFRP REINFORCEMENT

Construction using GFRP bars for reinforcement in concrete applications is similar to construction using steel reinforcement with some modifications. Unlike conventional steel reinforcement, GFRP reinforcing bars typically do not exhibit individually clear markings that identify the manufacturer, bar type, or bar size. This is lack of information typically a result of the manufacturing process. The ACI 440.1R-03 design and construction guidelines (2003) recommend that each producer label the solid bars or shipping container/packaging, or both, with a symbol identifying the manufacturer (XXX), type of fiber and nominal size (G for glass and number for nominal bar size, e.g., G#4), strength grade of the bar (e.g., F90 to indicate that the guaranteed tensile strength, $f_{fu}^{*}$, is greater than 90 ksi), and modulus grade (e.g., E5.5, indicating that the modulus of elasticity is at least 5,500 ksi). Bar sizes are the same as those listed in A615/A615M (2004), *Standard Specification for Deformed and Plain Billet-Steel Bars for Concrete Reinforcement*. Although bending GFRP bars is possible, due to the significant reduction in strength capacity caused by bending, most designs specify straight bars. Straight GFRP bars are typically ordered identifying length, guaranteed tensile strength, fiber type, diameter, and modulus of elasticity.

Significant differences between uncoated steel and GFRP reinforcing bars arise in handling and storage. GFRP bars should be handled in such ways as to eliminate or minimize surface damage, and storage conditions for GFRP bars should be controlled. The ACI 440.1R-03 design and construction guidelines recommend the following for GFRP bars:

- handle with work gloves;
- do not store on ground;
- exposure to high temperatures, ultraviolet rays, and chemical substances should be avoided;
- clean GFRP bar surfaces by wiping the bars with solvents if contaminated;
- if necessary, use a spreader bar for lifting; and

- if necessary, cut bars with high-speed grinder or fine-blade saw (bars should never be sheared).

The ACI design and construction guidelines provide further information and the reader is directed to this document if further information is needed. These practices should preserve the integrity of the GFRP bars.

In addition to handling and storage criteria for GFRP bars, guidance on the placement of GFRP is needed. GFRP bars can be placed in similar manners as that of steel reinforcing bars with the following additions and/or exceptions useful (ACI 440.1R-03 2003):

- requirements for chair placement should be included in project specifications;
- plastic or non-corrosive chairs are preferred;
- requirements for securing GFRP bars should be included in specifications to prevent movement of GFRP bars during concrete placement;
- site bending of thermoset GFRP bars is not allowed; and
- lapping of bars is necessary, and information on length of lap should be included in the specifications.

Figures 3 and 4 show GFRP rebar tying and chair placement and typical spacing for the Sierrita de las Cruz bridge construction outside of Amarillo, Texas. It can be seen that the GFRP bars were tied with coated wires (Figure 3) and typical chair spacing was approximately 3 ft. Actual chair spacing is dependent on bar type, tie requirements, and other parameters.

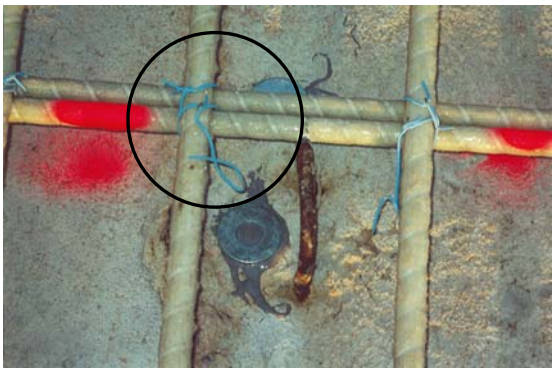

**Figure 3. Tying of GFRP Bars.**

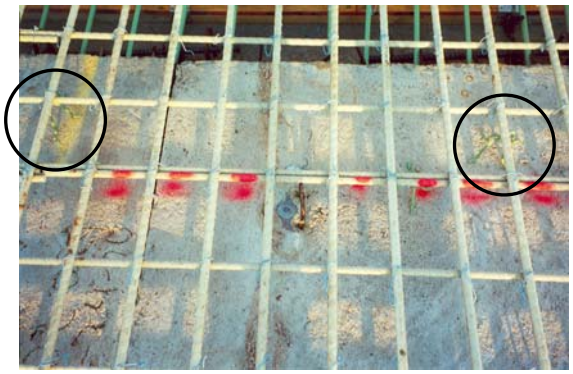

**Figure 4. Chair Placement for GFRP Reinforcement.**

# V. RECOMMENDED MAINTENANCE GUIDELINES FOR GFRP REINFORCED CONCRETE STRUCTURES

Several concrete structures have been constructed with GFRP reinforcement. Research results presented in Report 9-1520-3 (Trejo et al. 2003) indicate that GFRP bar strength, cracking of GFRP-reinforced concrete, and fatigue (both static and dynamic) could be critical issues associated with the use of GFRP bars in reinforced concrete systems. The authors of this report have clearly presented issues associated with the use of GFRP bars. In cases where GFRP bars have been used, personnel should evaluate the structure on a periodic basis to ensure structural integrity. Limited research or field work has been performed on maintenance and/or repair of GFRP-reinforced concrete members, and significant additional research is needed. However, the following issues should be evaluated and addressed as needed:

- cracking of the concrete;
- concrete spalling and delaminations;
- assessment of bar and member strength should be made, if tensile strength deterioration is expected;
- member deflections.

This is not an all-inclusive list. Other issues could arise, and these issues should be addressed using sound engineering judgment.

Maintenance of a GFRP-reinforced concrete member should include practices that reduce exposure of the GFRP reinforcing bars to saturated concrete conditions or to direct traffic. Maintenance should include sealing cracks and the concrete surface to prevent water ingress, repairing spalling or voids, and repairing and/or rehabilitating members as needed. Because previous research and field assessment of GFRP-reinforced concrete elements is limited, the engineer in charge should make maintenance and repair decisions as appropriate.

# VI. SUMMARY

This report provided an overview of the design, construction, and maintenance of bridge decks utilizing GFRP reinforcement. This overview is based on the observations and findings from research project 9-1520. It should be noted that these results were based on results from three different types of GFRP bars; each bar type from one manufacturing lot. Thus, the general recommendations provided herein are made with the assumption that the GFRP bars evaluated as part of research project 9-1520 were representative GFRP bars. If this is the case, the following design statements can be offered:

- Environmental reduction factors proposed by ACI may not be conservative.
- Cracking and deflection of GFRP-reinforced concrete are likely underestimated by ACI.
- The development length of straight GFRP bars is likely not conservative.
- Thermal mismatch of concrete and GFRP bars should be evaluated but does not seem to be as significant as originally believed.

GFRP reinforcing bars require special handling and storage procedures because surface damage can lead to reduced strengths and accelerated tensile strength deterioration of these bars. Bars should be stored such that exposure to high temperatures, ultraviolet rays, and chemical substances is avoided.

Minimal field work and research have been performed and, as a result, only limited recommendations can be made on the maintenance of GFRP-reinforced concrete sections. As with most concrete systems, crack, spalls, and delaminations should be repaired. Because this and other research has shown that GFRP bars deteriorate and can fail under static and dynamic fatigue conditions, the engineer or responsible party(ies) must evaluate the structure to determine capacity.

## REFERENCES


ACI Committee 440.1R-03, *Guide for the Design and Construction of Concrete with FRP Bars*, American Concrete Institute, Detroit, MI., 2003.

ACI Committee 318, "Building Code Requirements for Structural Concrete (ACI 318-99) and Commentary (318R-99)," American Concrete Institute, Farmington Hills, MI, April 2000, 391 pp.

AASHTO LRFD Bridge Design Specifications, 2nd Edition. American Association of State Highway and Transportation Officials, Washington, D.C., 1998.

Bakht, B., Al-Bazi, G., Banthia, N., Cheung, M., Erki, M. Faoro, M., Machida, A., Mufti, A. A., Neale, K. W., and Tadros, G., "Canadian Bridge Design Code Provisions for Fiber-Reinforced Structures," Journal of Composites for Construction, A.S.C.E., February 2000, pp. 3–15.

Beeby, A. W., "Corrosion of Reinforcing Steel in Concrete and Its Relation to Cracking," The Structural Engineer, V. 56, No. 3, March 1978, pp. 77–81.

Faza, S. S., and GangaRao, H. V. S., "Theoretical and Experimental Correlation of Behavior of Concrete Beams Reinforced with Fiber Reinforced Plastic Rebars," Fiber-Reinforced-Plastic Reinforcement for Concrete Structures, ACI Publication SP-138A, A. Nanni and C. W. Dolan, Eds., American Concrete Institute, Farmington Hills, MI, 1993, pp. 599–614.

Gilbert, R. I., and Mickleborough, N. C., *Design of Prestressed Concrete*, Unwin Hyman, London, 1990, 504 pp.

Glaser, R. E., Moore, R. L., and Chiao, T. T., "Life Estimation of an S-Glass/Epoxy Composite under Sustained Tensile Loading," Composites Technology Review, V. 5 No. 1, A.S.T.M., Philadelphia, PA, Spring 1983, pp. 21–26.

Naaman, A., and Jeong, S., "Structural Ductility of Concrete Beams Prestressed with FRP Tendons," Non-Metallic (FRP) Reinforcement for Concrete Structures, Proceedings of the Second International RILEM Symposium (FRPRCS-2), L. Taerwe, Ed., E and FN Spon, London, England, 1995, pp. 379–386.

Sen, R., Mullins, G., and Salem, T., "Durability of E-Glass Vinylester Reinforcement in Alkaline Solution," *ACI Structural Journal*, V. 99, No. 3, May-June 2002, pp. 369–375.

Trejo, D., Aguiñiga, F., Yuan, R. L., James, R. W., and Keating, P. B., Characterization of Design Parameters for Fiber Reinforced Polymer Composite Systems, Report FHWA/TX-04/1520-3, Texas Transportation Institute, College Station, TX, September 2003.

The American Society for Testing and Materials (ASTM), Standard Specification for Deformed and Plain Billet-Steel Bars for Concrete Reinforcement, A615/A615M, 2004.